Interactions and superconductivity in twisted an un-twisted graphene stacks









F.

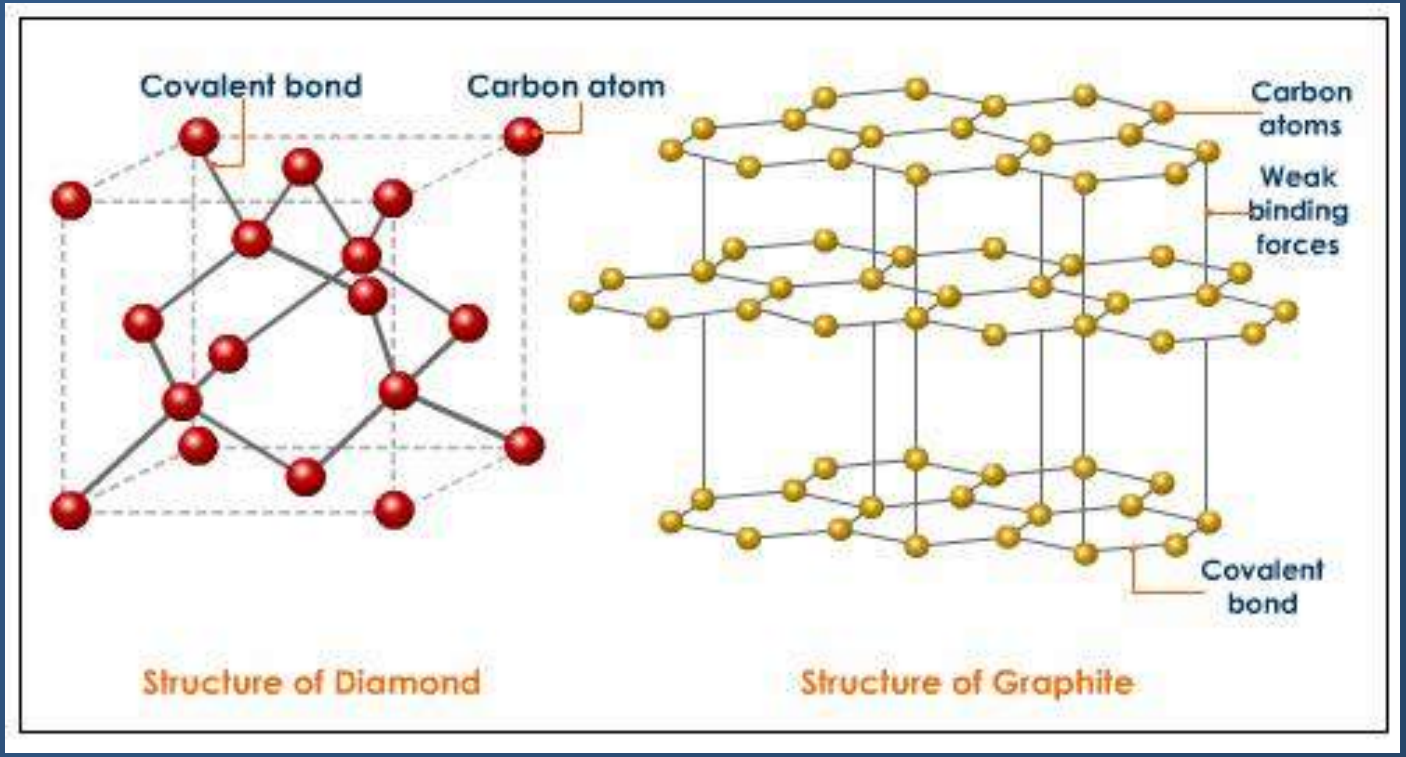
October 7th, 2026

Outline

- Interactions and phase diagram in twisted and un-twisted graphene bilayers
- Superconductivity in graphene stacks.
- Novel features in rhombohedral graphene.

In colaboration with N. R. Walet (U. Manchester), T. Cea, P. Pantaleon, A. Jimeno-Pozo, H. Sainz-Cruz, G. Parra, J. Silva (Imdea). Also V. P. Phong (U. Penn), V. Crépel, L. Fu, L. Levitov (MIT), Y. Oreg, E. Peleg. A. Stern (Weizmann), D. Kaplan (Rutgers), E. Mele (UPenn), A. Bernevig (Princeton, DIPC).

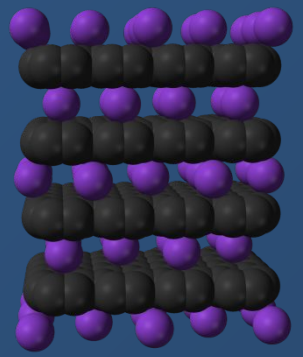
Graphene vs diamond



Related materials

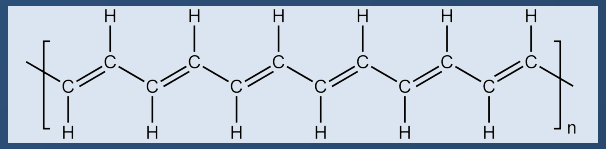
Graphite intercalation compounds:

- Doped graphene planes.
- Superconducting at low temperatures.



Polyacetylene:

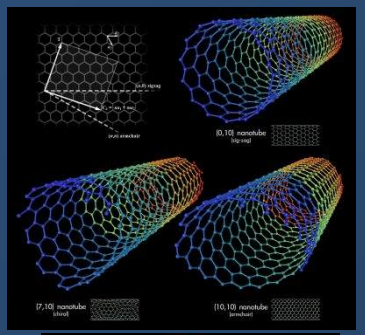
- π-bonded chain.
- Peierls distortion.



A. J. Heeger, A. G. MacDiarmid, H. Shirakawa, Nobel prize winners in Chemistry, 2000

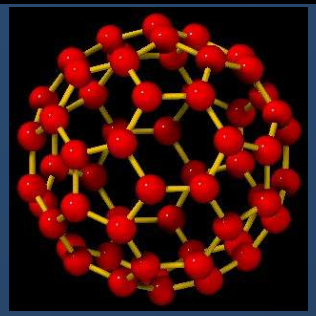
Nanotubes:

- superconducting and magnetic instabilities.



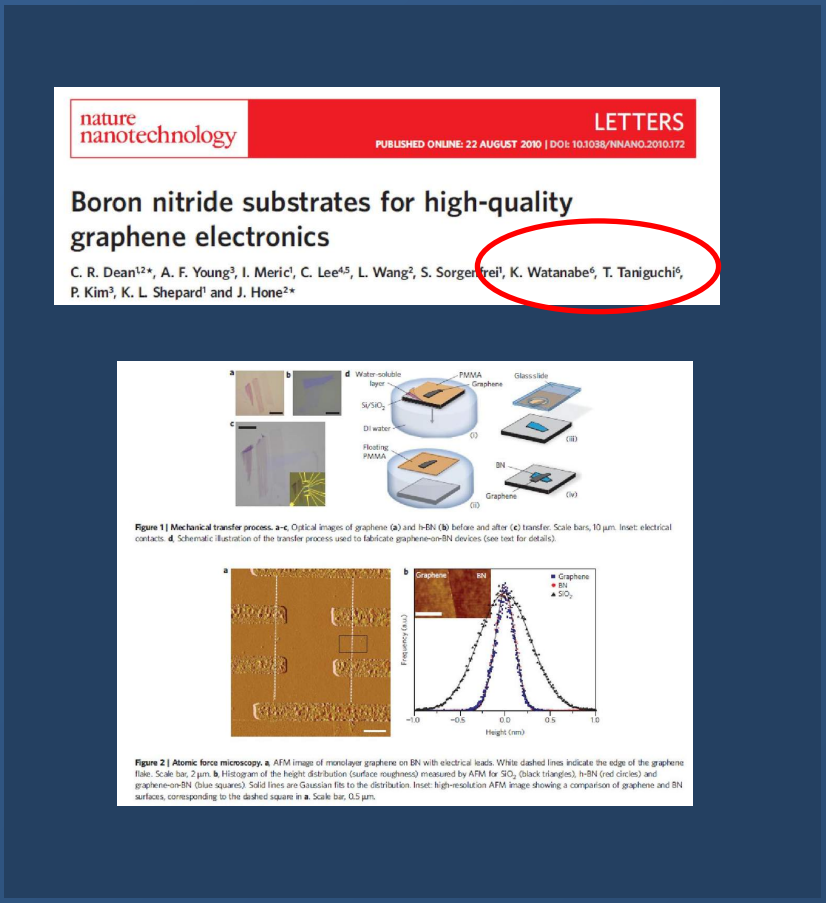
Fullerenes:

- superconducting when doped.



R. F. Curl Jr., H. W. Kroto, R. E. Smalley, Nobel prize winners in Chemistry, 1994

Hexagonal Boron Nitride, hBN



nature nanotechnology

LETTERS

PUBLISHED ONLINE: 22 AUGUST 2010 | DOI: 10.1038/NNANO.2010.172

Boron nitride substrates for high-quality graphene electronics

C. R. Dean[1,2]*, A. F. Young[3], I. Meric[1], C. Lee[4,5], L. Wang[2], S. Sorgenfrei[1], K. Watanabe[6], T. Taniguchi[6], P. Kim[3], K. L. Shepard[1] and J. Hone[2]*

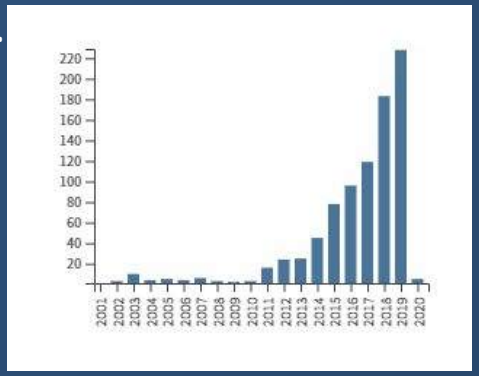
Figure 1 | Mechanical transfer process. a–c, Optical images of graphene (**a**) and h-BN (**b**) before and after (**c**) transfer. Scale bars, 10 μm. Inset: electrical contacts. **d**, Schematic illustration of the transfer process used to fabricate graphene-on-BN devices (see text for details).

Figure 2 | Atomic force microscopy. a, AFM image of monolayer graphene on BN with electrical leads. White dashed lines indicate the edge of the graphene flake. Scale bar, 2 μm. **b**, Histogram of the height distribution (surface roughness) measured by AFM for SiO_2 (black triangles), h-BN (red circles) and graphene-on-BN (blue squares). Solid lines are Gaussian fits to the distribution. Inset: high-resolution AFM image showing a comparison of graphene and BN surfaces, corresponding to the dashed square in **a**. Scale bar, 0.5 μm.

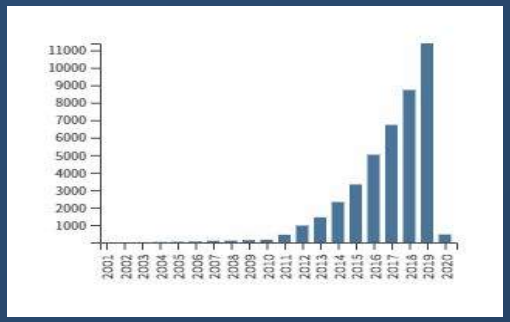
- Honeycomb lattice
- Lattice constant 2% larger tha graphene's

Web of Science statistics:

Taniguchi, T. and Watanabe K.



Total publications per year



Sum of times cited per year

Graphene on a substrate: Moiré structure

PRL 100, 056807 (2008) PHYSICAL REVIEW LETTERS week ending 8 FEBRUARY 2008

Periodically Rippled Graphene: Growth and Spatially Resolved Electronic Structure

A. L. Vázquez de Parga,[1] F. Calleja,[1] B. Borca,[1] M. C. G. Passeggi, Jr.,[2] J. J. Hinarejos,[1] F. Guinea,[3] and R. Miranda[1,4]

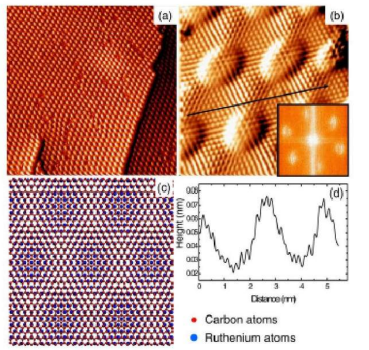


FIG. 1 (color online). (a) 76 nm × 76 nm STM image of graphene/Ru(0001) showing the decoration of a screw dislocation and a monoatomic step from the substrate. There are also some defects on the rippled structure. (b) 6.5 nm × 6.5 nm atomically resolved image of graphene/Ru(0001). The image was taken with a sample bias voltage of $V_s = -4.5$ mV and a tunnel current of $I_t = 3$ nA. The image is differentiated along the X direction in order to see the weak atomic corrugation superimposed to the ripples. The inset reproduces the Fourier transform of the image showing the (11 × 11) periodicity of the rippled graphene layer. The larger hexagonal pattern corresponds to the C-C distances and the smaller spots to the periodic ripples. (c) Corresponding structural model. (d) Line profile marked with an arrow in panel (b). The atomic corrugation in these conditions is around 5 pm.

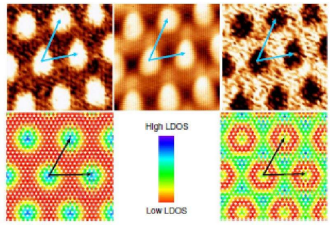


FIG. 3 (color online). The left and right images in the upper panel are maps of dI/dV at −100 meV and +200 meV and reflects the spatial distribution of the LDOS below and above the Fermi level, respectively, for an extended graphene layer on Ru(0001). The central image shows the topographic image recorded simultaneously. The lower panel shows the corresponding calculations for the spatially resolved LDOS for a (11 × 11) periodically corrugated graphene layer.

LETTERS
PUBLISHED ONLINE: 13 FEBRUARY 2011 | DOI: 10.1038/NMAT2968
nature materials

Scanning tunnelling microscopy and spectroscopy of ultra-flat graphene on hexagonal boron nitride

Jiamin Xue[1], Javier Sanchez-Yamagishi[2], Danny Bulmash[2], Philippe Jacquod[1,3], Aparna Deshpande[11], K. Watanabe[4], T. Taniguchi[4], Pablo Jarillo-Herrero[2] and Brian J. LeRoy[1]*

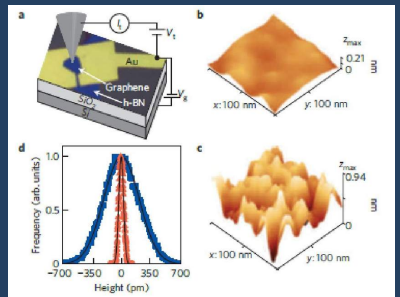


Figure 1 | Schematic device set-up and topography comparison of graphene on hBN and SiO_2. **a**, Optical microscope image of the mechanically exfoliated monolayer graphene flake with hBN underneath and gold electrodes contacting it above. The wiring of the STM tip and back gate voltage is indicated. **b**, STM topographic image of monolayer graphene on hBN showing the underlying surface corrugations. The image is 100 nm × 100 nm. The imaging parameters are tip voltage $V_t = -0.3$ V, tunnelling current $I_t = 100$ pA. **c**, STM topographic image of monolayer graphene on SiO_2 showing markedly increased corrugations. The imaging parameters are tip voltage $V_t = -0.5$ V, tunnelling current $I_t = 50$ pA. **d**, Histogram of the height distributions for graphene on SiO_2 (blue squares) and graphene on hBN (red triangles) along with Gaussian fits.

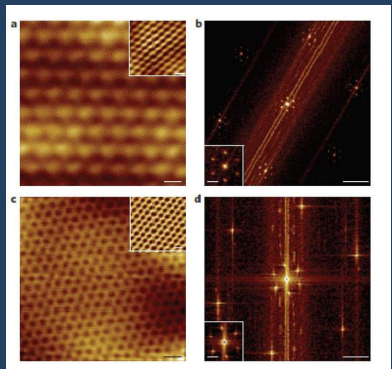


Figure 2 | Real space and Fourier transforms of Moiré patterns a, STM topographic images of a Moiré pattern produced by graphene on hBN. The scale bar is 2 nm. The inset is a zoom in of a 2 nm region with a scale bar of 0.3 nm. The imaging parameters are $V_t = -0.3$ V and $I_t = 100$ pA. **b**, Fourier transform of **a** showing the six graphene lattice points near the edge of the image and the long wavelength Moiré pattern near the centre of the image and around each lattice point. The scale bar is 10 nm^{-1}. The inset is a zoom in around one of the lattice points with a scale bar of 2 nm^{-1}. **c**, STM topographic image from another region of the same graphene flake showing a different Moiré pattern. The scale bar is 2 nm. The inset is a zoom in of a 2 nm region with a scale bar of 0.3 nm. The imaging parameters are $V_t = -0.3$ V and $I_t = 100$ pA. **d**, Fourier transform of **c** showing the atomic lattice as well as the Moiré pattern. The scale bar is 10 nm^{-1}. The inset is a zoom of the Moiré pattern with a scale bar of 4 nm^{-1}.

Superconductivity in graphene

Superconductivity in graphene. March Meeting, Los Angeles 2018

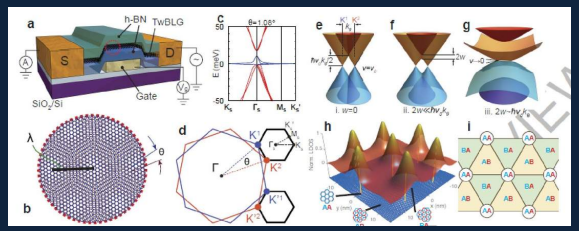
nature Accelerated Article Preview

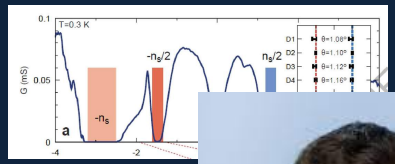
LETTER

doi:10.1038/nature26154

Correlated insulator behaviour at half-filling in magic-angle graphene superlattices

Yuan Cao, Valla Fatemi, Ahmet Demir, Shiang Fang, Spencer L. Tomarken, Jason Y. Luo, J. D. Sanchez-Yamagishi, K. Watanabe, T. Taniguchi, E. Kaxiras, R. C. Ashoori & P. Jarillo-Herrero







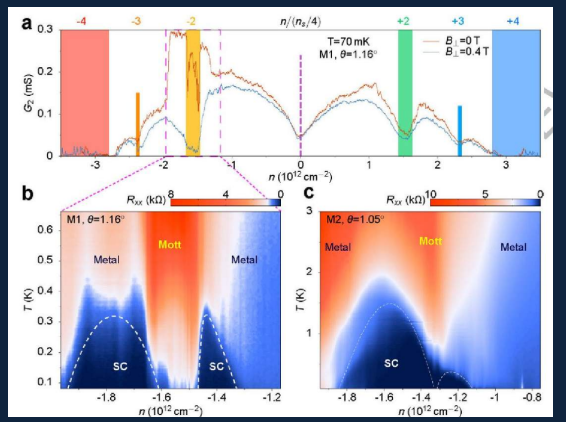
nature Accelerated Article Preview

ARTICLE

doi:10.1038/nature26160

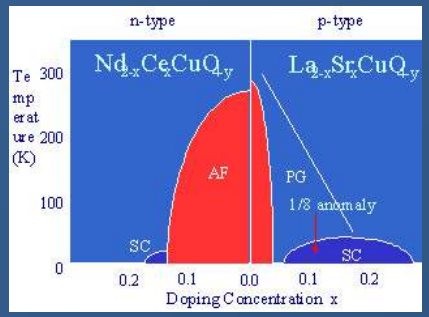
Unconventional superconductivity in magic-angle graphene superlattices

Yuan Cao, Valla Fatemi, Shiang Fang, Kenji Watanabe, Takashi Taniguchi, Efthimios Kaxiras & Pablo Jarillo-Herrero

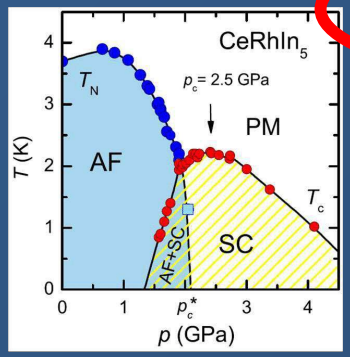


Pablo Jarillo-Herrero, MIT Cambridge, USA

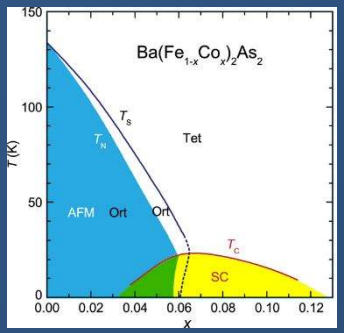
Strongly correlated systems



Cuprate superconductors



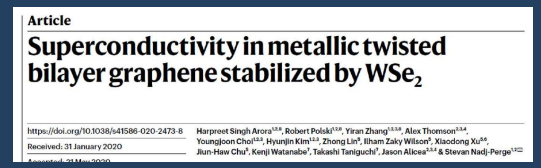
Heavy fermion compounds



Pnictides

Pairing due to magnetic fluctuations
Variations of the Hubbard model

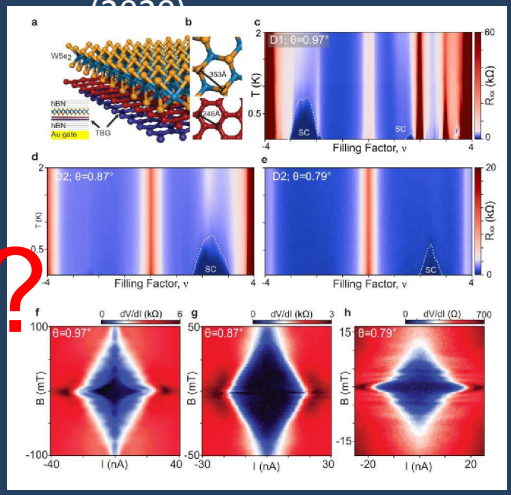
?



Article

Superconductivity in metallic twisted bilayer graphene stabilized by WSe_2

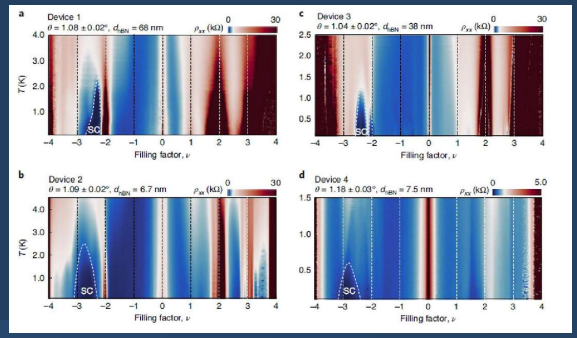
Nature **583**, 579 (2020)



Independent superconductors and correlated insulators in twisted bilayer graphene

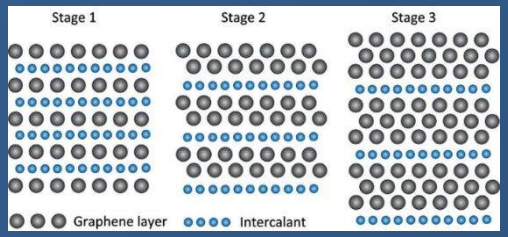
Yu Saito[1], Jingyuan Ge[2], Kenji Watanabe[3], Takashi Taniguchi[3] and Andrea F. Young[2]

Nature Phys. **16**, 926

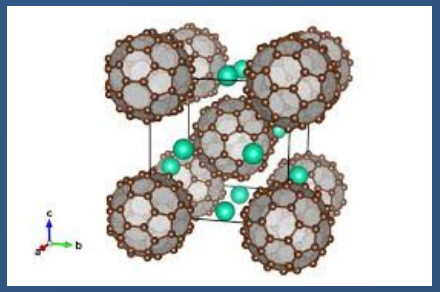


Superconductivity and strongly correlated phases in carbon compounds

Superconductivity



Graphite intercalation compounds, such as C_6Ca, $n \geq 10^{14}\ \mathrm{cm}^{-2}, T_c \sim 1 - 10\mathrm{K}$



Alkali intercalated fullerenes, such as Rb_3C_{60}, $T_c \sim 10 - 40\mathrm{K}$

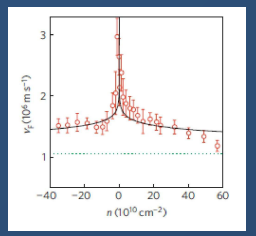
Renormalization of the Fermi velocity

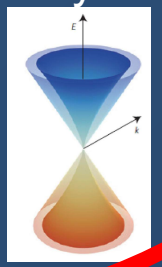
nature physics — LETTERS

PUBLISHED ONLINE: 24 JULY 2011 | DOI: 10.1038/NPHYS2049

Dirac cones reshaped by interaction effects in suspended graphene

D. C. Elias[1], R. V. Gorbachev[1], A. S. Mayorov[1], S. V. Morozov[2], A. A. Zhukov[2], P. Blake[3], L. A. Ponomarenko[1], I. V. Grigorieva[1], K. S. Novoselov[1], F. Guinea[4]* and A. K. Geim[1,3]



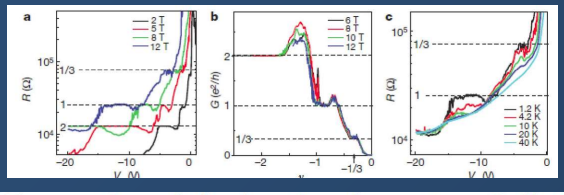


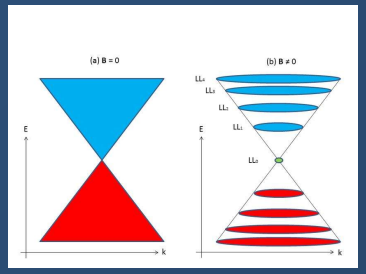
Landau levels

Fractional quantum Hall effect and insulating phase of Dirac electrons in graphene

Xu Du[1]†, Ivan Skachko[1], Fabian Duerr[1], Adina Luican[1] & Eva Y. Andrei[1]

Nature **462**, 192 (2009)

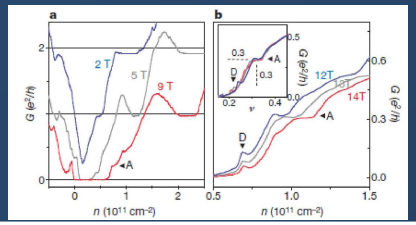




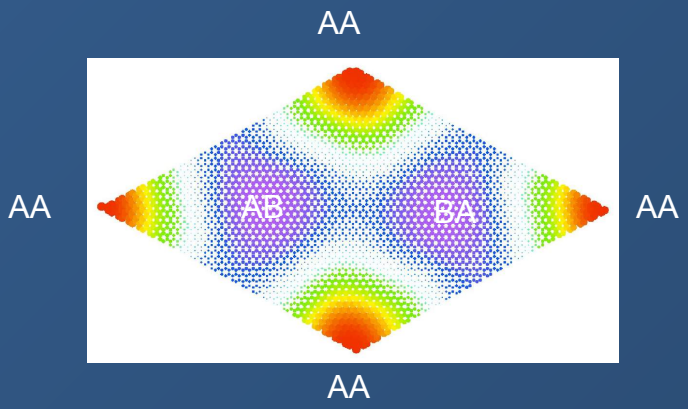
Observation of the fractional quantum Hall effect in graphene

Kirill I. Bolotin[1]*†, Fereshte Ghahari[1]*, Michael D. Shulman[2], Horst L. Stormer[1,2] & Philip Kim[1,2]

Nature **462**, 196 (2009)



Interactions in twisted bilayer graphene

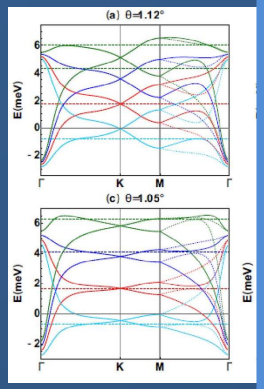


Number of atoms:		
Moiré unit length:		
Radius of the charge distribution:		
Coulomb energy:		
Intraatomic (Hubbard) repulsion:		
Electron-phonon coupling, LA:		
Electron-phonon coupling, TA:		

Shapes and widths of the bands: theory

PHYSICAL REVIEW B **100**, 205113 (2019)

Electronic band struct

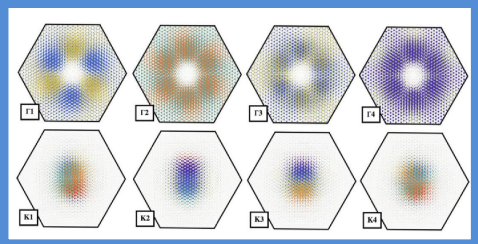


$V_H(AA) - V_I$

PHYSICAL REVIEW B **98**, 235158 (2018)

Charge-transfer insulation in twisted bilayer graphene

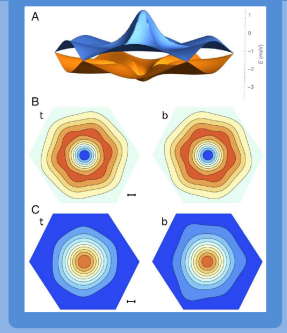
Louk Rademaker[1,2] and Paula Mellado[2,3]

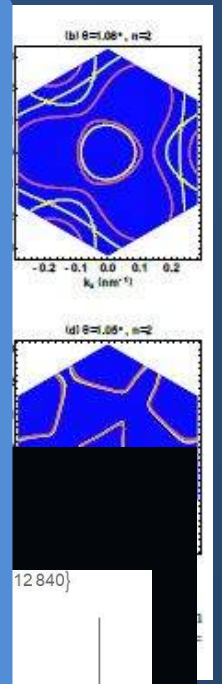


Electrostatic effects, band distortions, and superconductivity in twisted graphene bilayers

Francisco Guinea[a,b,1,2] and Niels R. Walet[b,1,2]

13174–13179 | PNAS | December 26, 2018 | vol. 115 | no. 52



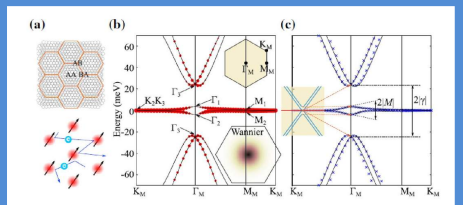


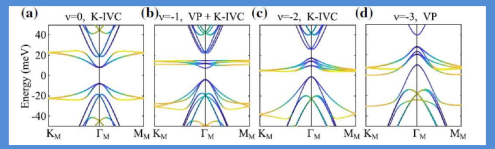
PHYSICAL REVIEW LETTERS **129**, 047601 (2022)

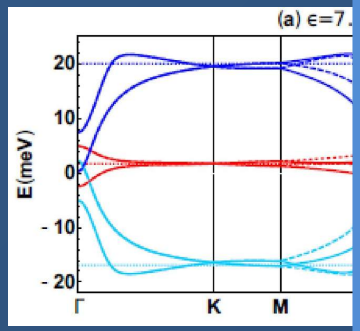
Editors' Suggestion | Featured in Physics

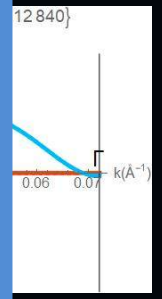
Magic-Angle Twisted Bilayer Graphene as a Topological Heavy Fermion Problem

Zhi-Da Song[1,2,*] and B. Andrei Bernevig[2,3,4]









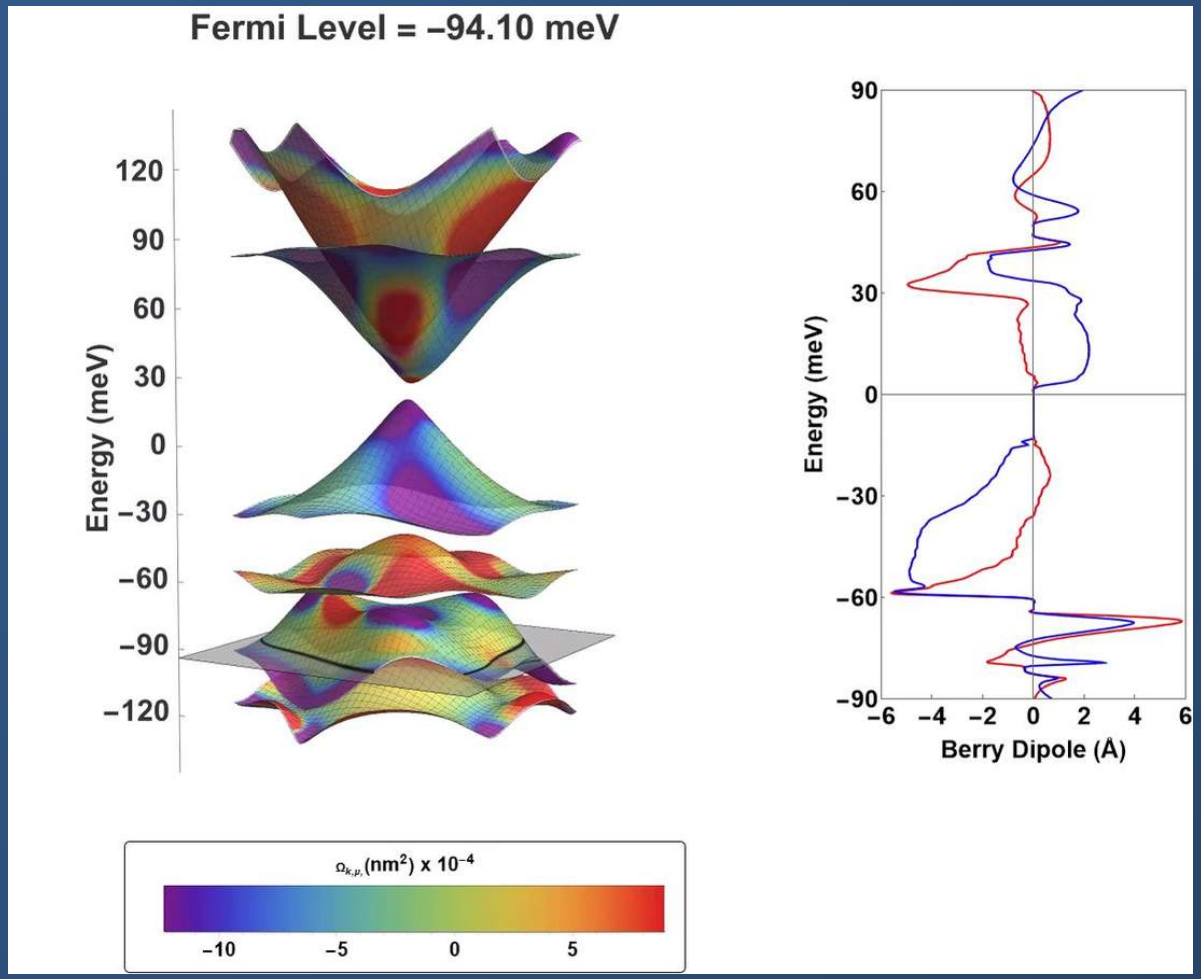
he density of
states at the Fermi energy remains high (pinning of
van Hove singularities).

PHYSICAL REVIEW B **106**, L161101 (2022)

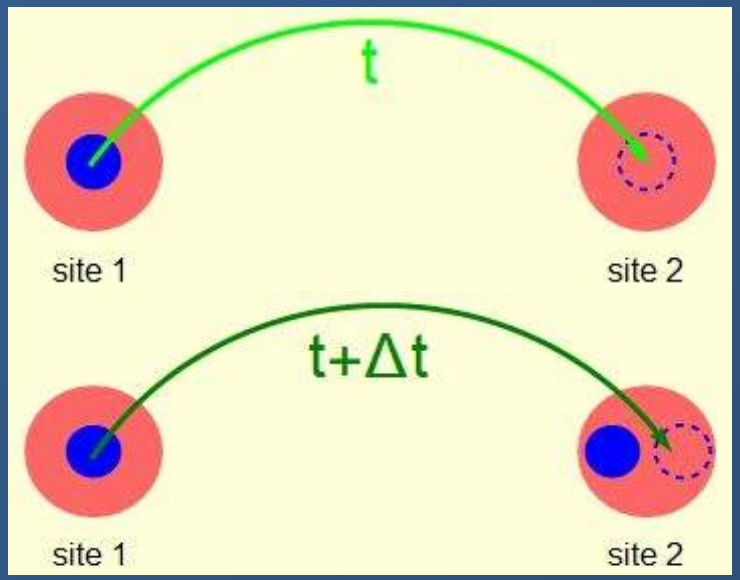
Letter

Interaction-enhanced topological Hall effects in strained twisted bilayer graphene

Pierre A. Pantaleón,[1,*] Võ Tiến Phong,[2,†] Gerardo G. Naumis,[3] and Francisco Guinea[1,4,5]



Electron assisted hopping



PROCEEDINGS OF THE ROYAL SOCIETY A MATHEMATICAL, PHYSICAL & ENGINEERING SCIENCES

On the Electron Theory of Metals

S. Schubin and S. Wonsowsky

Proc. R. Soc. Lond. A 1934 **145**, doi: 10.1098/rspa.1934.0089, published 2 June 1934

J. Phys. C: Solid State Phys., Vol. 12, 1979. Printed in Great Britain. © 1979

Some types of instabilities in the electron energy spectrum of the polar model of the crystal: I. The maximum-polarity state

S V Vonsovsky and M I Katsnelson

PHYSICAL REVIEW B VOLUME 41, NUMBER 10 1 APRIL 1990

Hole superconductivity and the high-T_c oxides

F. Marsiglio and J. E. Hirsch

41 6435 ©1990 The American Physical Society

Cascade of phase transitions in twisted bilayer graphene

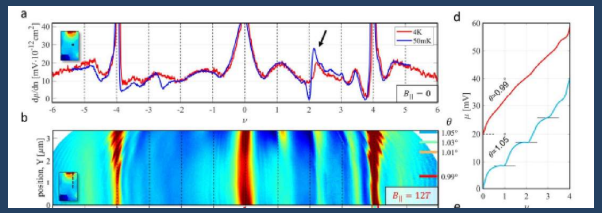
Article

Cascade of phase transitions and Dirac revivals in magic-angle graphene

https://doi.org/10.1038/s41586-020-2373-y
Received: 25 November 2019

U. Zondiner[1,5], A. Rozen[1,5], D. Rodan-Legrain[1,5], Y. Cao[1], R. Queiroz[2], T. Taniguchi[3], K. Watanabe[4], Y. Oreg[2], F. von Oppen[2], Ady Stern[2], E. Berg[2], P. Jarillo-Herrero[1]✉ & S. Ilani[1]✉

Nature **582**, 203 (2020).

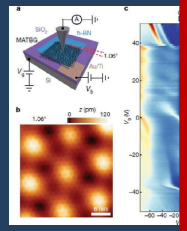


Article

Cascade of electro… magic-angle twist…

https://doi.org/10.1038/s41586-020-2339-0

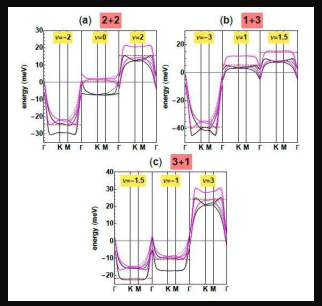
Nature **58**…



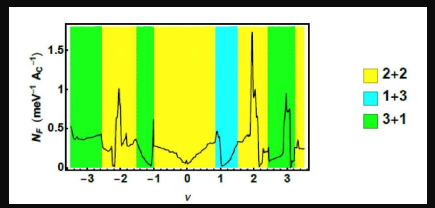
PHYSICAL REVIEW B **102**, 045107 (2020)

Band structure and insulating states driven by Coulomb interaction in twisted bilayer graphene

Tommaso Cea[1] and Francisco Guinea[1,2]



The mean field (HF) cascade



LETTERS
https://doi.org/10.1038/s41567-021-01347-4
nature physics

Unconventional sequence of correlated Chern

Chern insulators, van Hove singularities and



Douglas R. Hartree



Vladimir A. Fock

- The long range Coulomb interaction gives a qualitative explanation of the band deformations, and of the broken symmetry phases of twisted bilayer graphene.
- It does not identify details of the broken symmetry phases.

Superconductivity in twisted bilayer graphene. Some theoretical models

Electron-phonon coupling:

F. Wu, E. Hwang, S. Das Sarma, Phys. Rev. B 99, 165112 (2019)
F. Wu, A. H. MacDonald, I. Martin, Phys. Rev. Lett. 121, 257001 (2018)
B. Lian, Z. Wang, B. A. Bernevig, Phys. Rev. Lett. 122, 257002 (2019)

Electron-electron coupling: effect of van Hove singularities:

Y. Lin, R. M. Nandkishore, Phys. Rev. B 98, 214521 (2018)

T. Cea, F. G., Proc. Nat. Acad. Sci. **118**, e2107874118 (2021)
V. T. Phong, P. A. Pantaleon, T. Cea, F. G., Phys. Rev. B **104**, L121116 (2022)
T. Cea, P. A. Pantaleon, V. T. Phong, F. G., Phys. Rev. B **105**, 075432 (2022)
A. Jimeno-Pozo, H. Sainz-Cruz, T. Cea, P. Pantaleon, F. G., Phys. Rev. B **107**, L161106 (2023)
H. Sainz-Cruz, P. A. Pantaleon, F. G., Phys. Rev. Lett. **131**, 016003 (2023)
V. T. Phong, H. Sainz-Cruz, E. J. Mele, F. G., Phys. Rev. B **110**, L100501 (2024)
M. Long, A. Jimeno-Pozo, H. Sainz-Cruz, P. A. Pantaleon, F. G., Proc. Nat. Acad. Sci. **121**, e2405259121 (2024)

Coulomb interaction:

T. Cea, F. G., Proc. Nat. Acad. Sci. 118, e2107874118 (2021)
G. Savit, E. Berg, A. Stern, Y. Oreg, Phys. Rev. Lett. 127, 247703 (2022)
V. Kozii, M. P. Zaletel, N. Bultnick, Phys. Rev. B 106, 235157 (2022)

Long range interactions and superconductivity: the Kohn-Luttinger mechanism

NEW MECHANISM FOR SUPERCONDUCTIVITY*

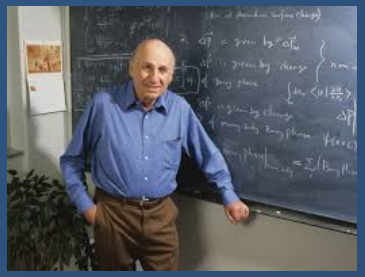
W. Kohn

University of California, San Diego, La Jolla, California

and

J. M. Luttinger

Phys. Rev. Lett. **15**, 524 (1965)



Walter Kohn



Joaquin M. Luttinger

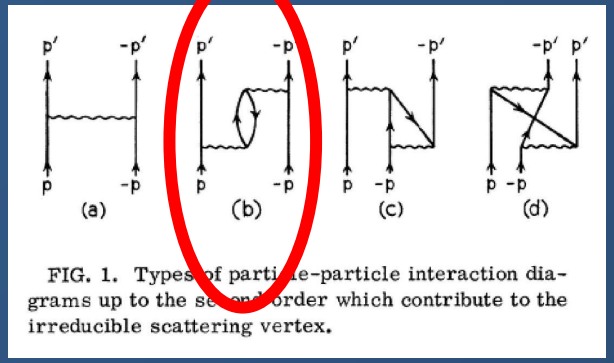


FIG. 1. Types of particle-particle interaction diagrams up to the second order which contribute to the irreducible scattering vertex.

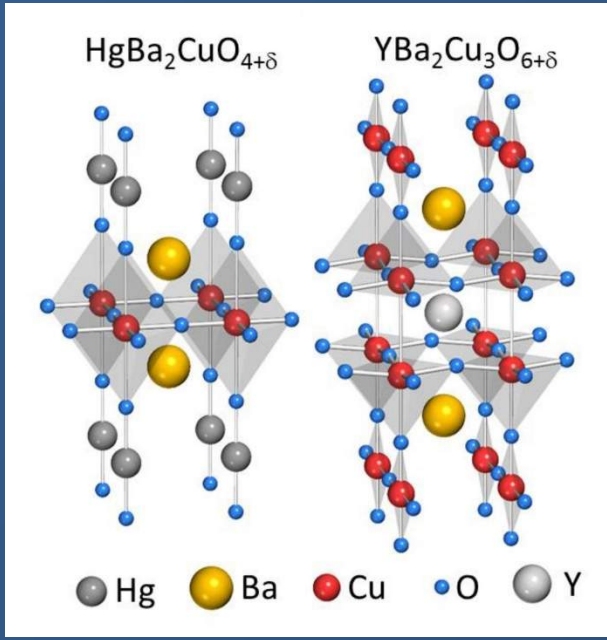
Superconductivity mediated by electron-hole pairs

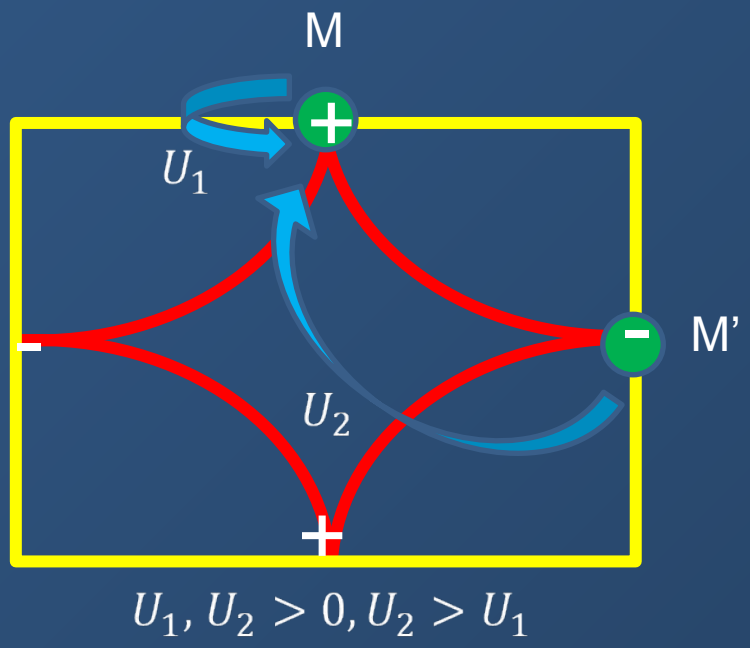
For electrons in metals we can make estimates using a screening Coulomb potential. It is easily seen that in the high-density limit $u(0)$ dominates and becomes $u(0) = \pi^2/mk_F$; therefore,

$$(kT_c/\epsilon_0) \sim \exp[-(2l)^4].$$

We also mention that since the electron-phonon interaction is screened by the same kind of mechanism, it too should contribute to long-range effects.

d-wave superconductivity in cuprates





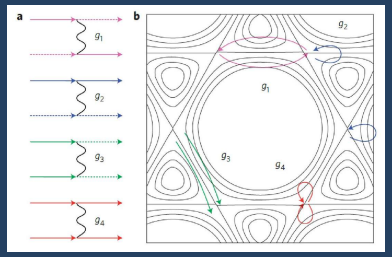
For electrons in metals we can make estimates using a screening Coulomb potential. It is easily seen that in the high-density limit $u(0)$ dominates and becomes $u(0) = \pi^2/mk_F$; therefore,

$$(kT_c/\epsilon_0) \sim \exp[-(2l)^4].$$

ARTICLES
PUBLISHED ONLINE: 22 JANUARY 2012 | DOI: 10.1038/NPHYS2208
nature physics

Chiral superconductivity from repulsive interactions in doped graphene

Rahul Nandkishore[1], L. S. Levitov[1] and A. V. Chubukov[2]*



Electron assisted hopping, a simple model

SCIENCE ADVANCES | RESEARCH ARTICLE

MATERIALS SCIENCE

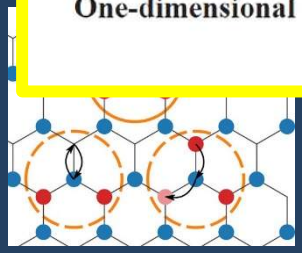
New mechanism and exact theory of superconductivity from strong repulsive interaction

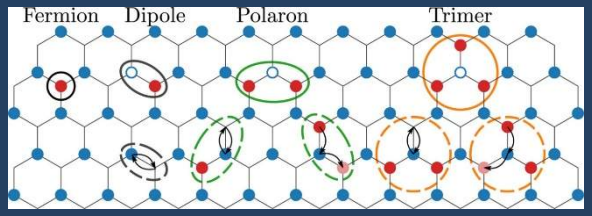
Valentin Crépel* and Liang Fu*

Sci. Adv. 2021; 7 : eabh2233 23 July 2021

$$\mathcal{H} = -t \sum_{\langle r,r' \rangle} \left(c_r^\dagger c_{r'} + h.c. \right) + \Delta \sum_{r \in B} n_r + V \sum_{\langle r,r' \rangle} n_r n_{r'}$$

Spinless electrons in the (sublattice polarized) honeycomb la





PHYSICAL REVIEW B, VOLUME 64, 033102

One-dimensional spinless fermion model with competing interactions beyond half filling

A. K. Zhuravlev and M. I. Katsnelson

PHYSICAL REVIEW B **105**, 094506 (2022)

Editors' Suggestion | Featured in Physics

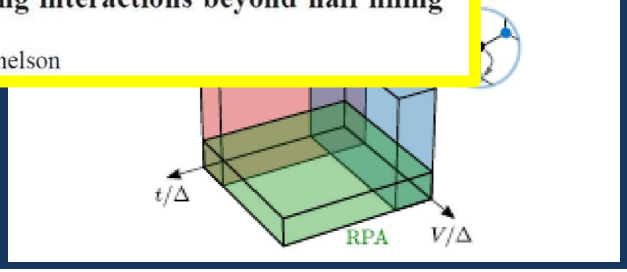
Unconventional superconductivity due to interband polarization

Valentin Crépel,[1] Tommaso Cea,[2] Liang Fu,[1] and Francisco Guinea[2,3,4]

Physics

Explaining Superconductivity in 2D Materials

Interactions between electrons in multiple electronic bands can produce a strong coupling among electrons—providing the "glue" that holds



- Simple model of a superconductor by repulsive interactions
- p-wave
- Finite gap, with opposite signs at the two valleys

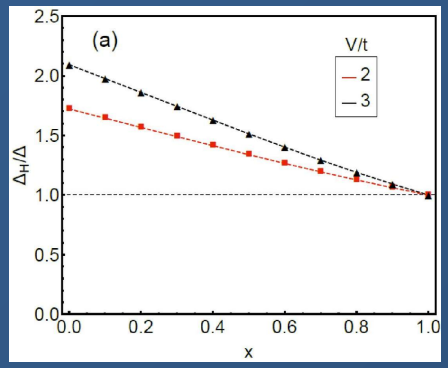
Results

PHYSICAL REVIEW B **105**, 094506 (2022)

Editors' Suggestion | Featured in Physics

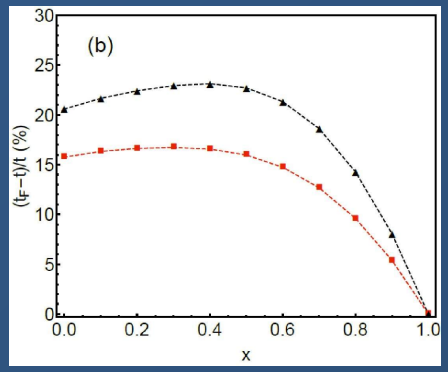
Unconventional superconductivity due to interband polarization

Valentin Crépel,[1] Tommaso Cea,[2] Liang Fu,[1] and Francisco Guinea[2,3,4]

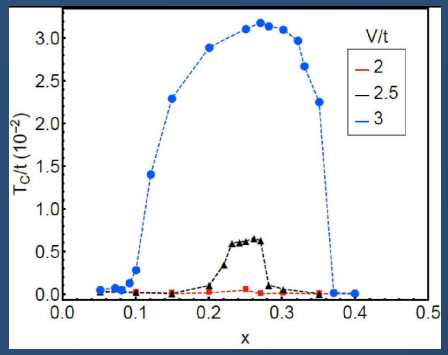


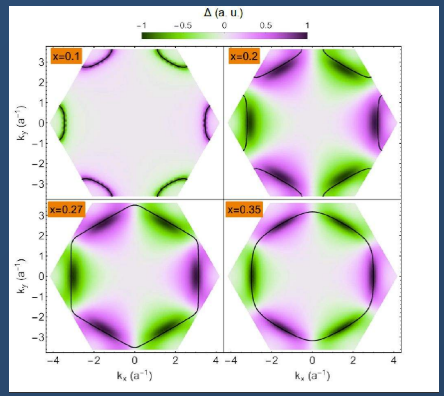
$$\tilde{\mathcal{H}} = \sum_{\vec{k},\sigma,\tau} \frac{\left|\vec{k}\right|^2}{2m} \psi^{\dagger}_{\vec{k},\sigma,\tau} \psi_{\vec{k},\sigma,\tau} + \frac{g_0}{N_f} \sum_{\vec{q}} \rho_{\vec{q}} \rho_{-\vec{q}}$$

$$g_0 = -\frac{27t^2V^2}{N_f(\Delta + 3V)^3}$$



- Nodeless superconductivity
- Attraction at small momenta



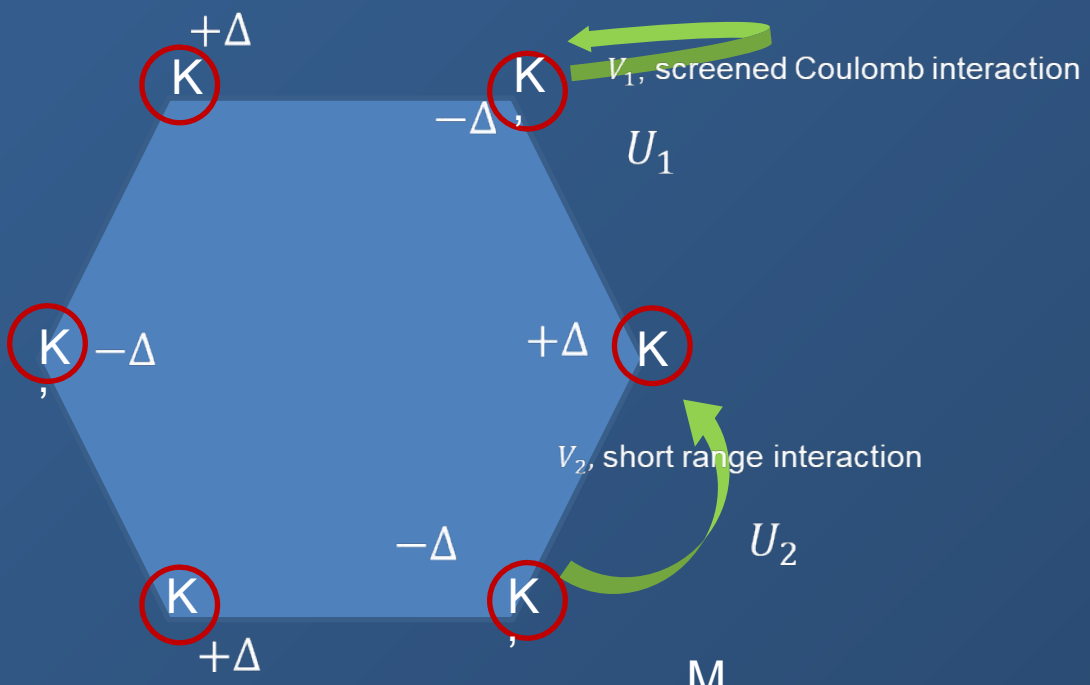


Hartree-Fock

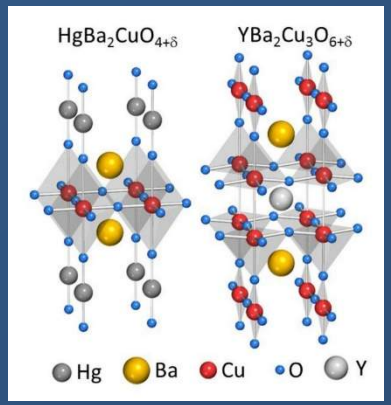
$\Delta/t=10$

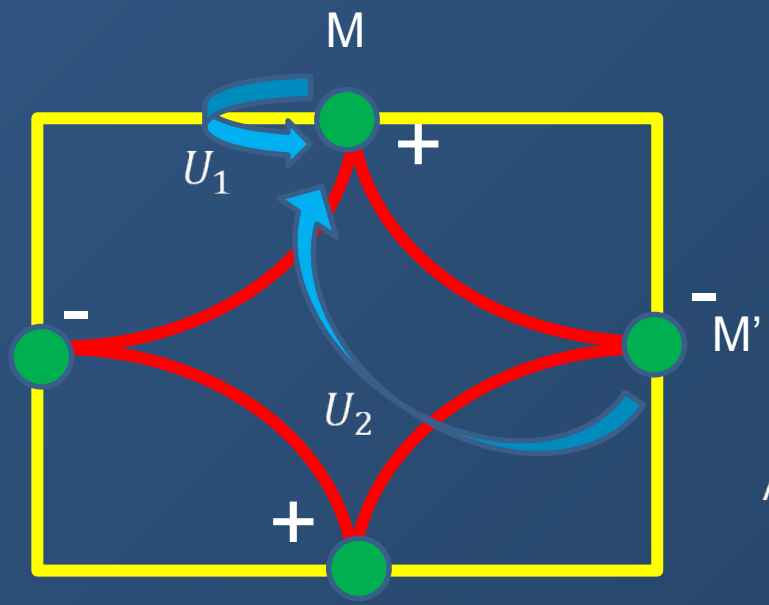
Superconductivity

f-wave superconductivity



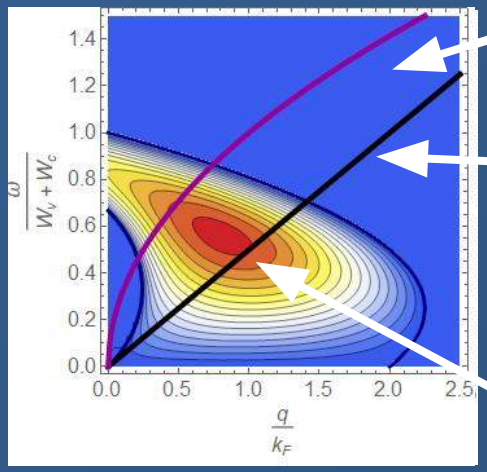
$$U_1, U_2 > 0, U_2 > U_1$$

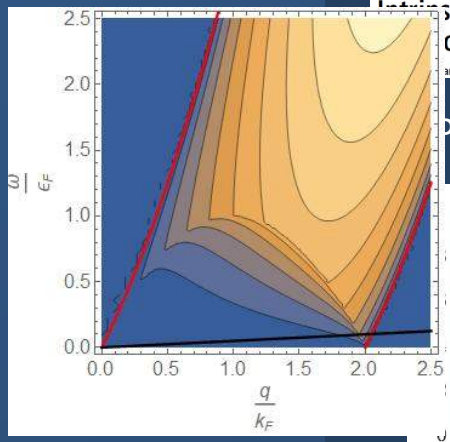




Also $p_{\pm}$ superconductivity in pnictide

Low energy excitations and charge excitations: Electron-hole pairs, plasmons, and phonons

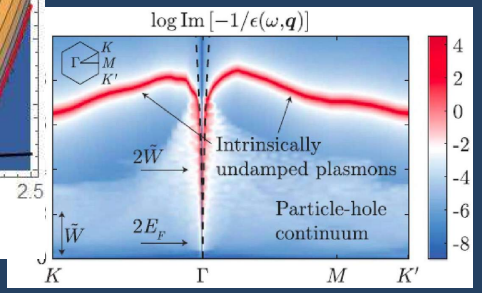




sically undamped plasmon modes in narrow on bands

ndowski[a,1] and Leonid Levitov[a]

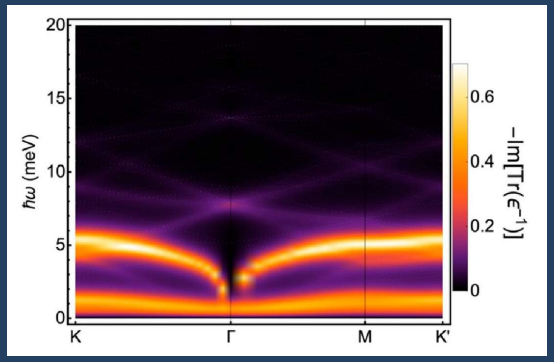
PNAS **116**, 20829 (2019)



Coulomb interaction, phonons, and superconductivity in twisted bilayer graphene

Tommaso Cea[a,b] and Francisco Guinea[a,c,d,1]

PNAS **118**, e2107874118 (2021)

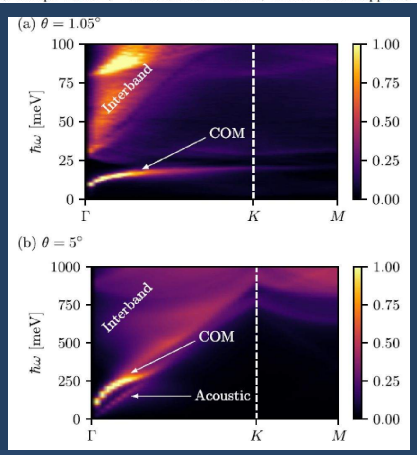


PHYSICAL REVIEW B **110**, 045431 (2024)

Editors' Suggestion | Featured in Physics

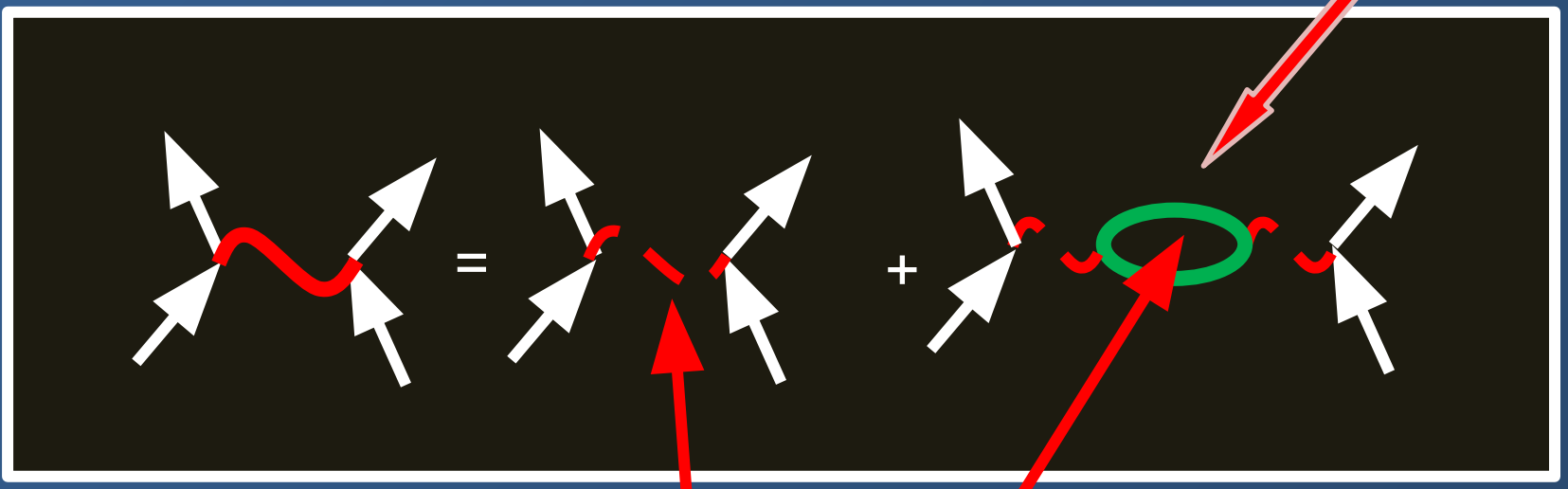
Theory of intrinsic acoustic plasmons in twisted bilayer graphene

Lorenzo Cavicchi[1], Iacopo Torre[2,3], Pablo Jarillo-Herrero,[4] Frank H. L. Koppens,[3,5] and Marco Polini[3,6]



Repulsive interactions and pairing

RPA resummation



- Longitudinal phonons modify the susceptibility.
- The bare interaction is the repulsive Coulomb coupling

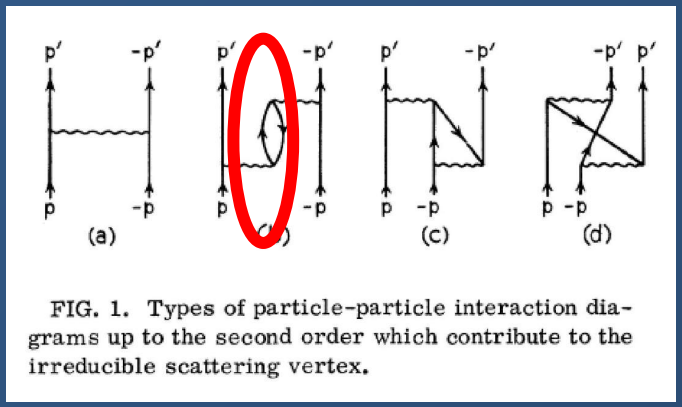


FIG. 1. Types of particle-particle interaction diagrams up to the second order which contribute to the irreducible scattering vertex.

NEW MECHANISM FOR SUPERCONDUCTIVITY*

W. Kohn

University of California, San Diego, La Jolla, California

and

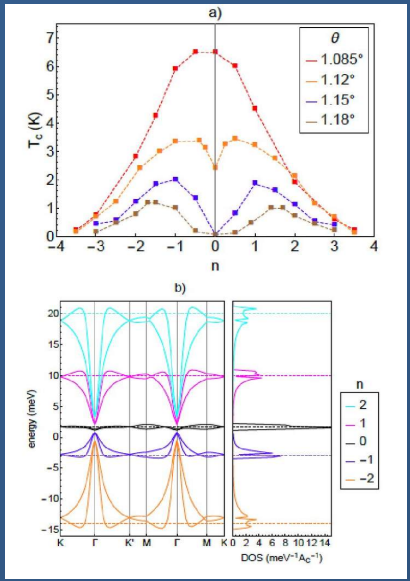
J. M. Luttinger

Phys. Rev. Lett. **15**, 524 (1965)

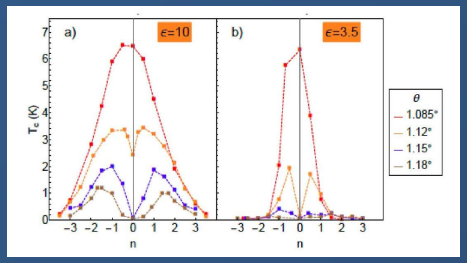
We also mention that since the electron-phonon interaction is screened by the same kind of mechanism, it too should contribute to long-range effects.

Results: critical temperature

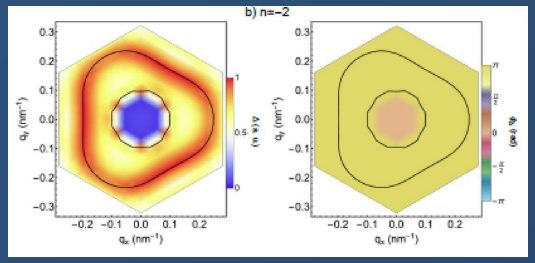
Critical temperatures



Bands, densities of states, magic angle



Dependence on dielectric constant



- Order parameter. Finite gap in each valley
- Consistent with spin singlet/valley triplet or with spin triplet/valley singlet superconductivity.

- The critical temperature is significantly enhanced by the electron-phonon interaction.
- Superconductivity correlates with the density of states at the Fermi level.
- The effect of external screening depends on the strength of the electron-phonon interaction.

Superconductivity in twisted trilayers

Article

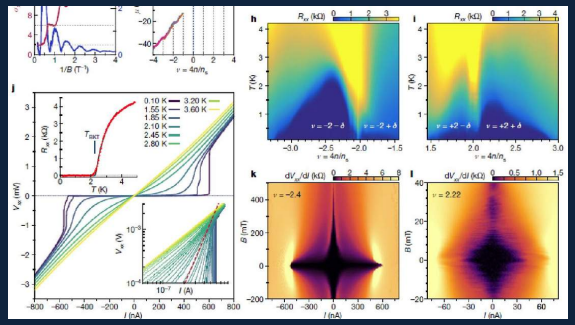
Tunable strongly coupled superconductivity in magic-angle twisted trilayer graphene

https://doi.org/10.1038/s41586-021-03192-0
Received: 26 October 2020

Jeong Min Park[1,4], Yuan Cao[1,4✉], Kenji Watanabe[2], Takashi Taniguchi[3] & Pablo Jarillo-Herrero[1✉]

Nature | Vol 590 | 11 February 2021 | 249



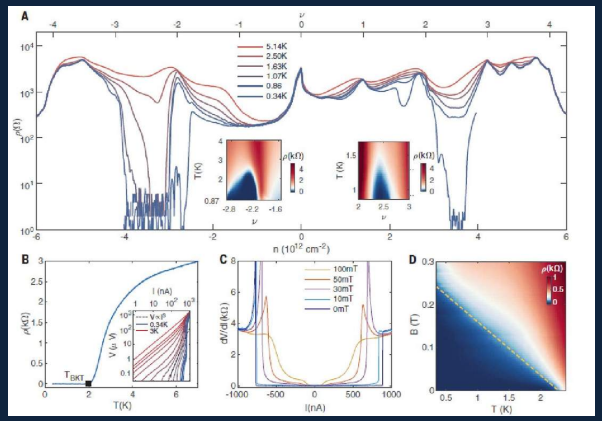


SUPERCONDUCTIVITY

Electric field–tunable superconductivity in alternating-twist magic-angle trilayer graphene

Zeyu Hao[1]*, A. M. Zimmerman[1]*, Patrick Ledwith[1], Eslam Khalaf[1], Danial Haie Najafabadi[1], Kenji Watanabe[2], Takashi Taniguchi[3], Ashvin Vishwanath[1], Philip Kim[1]†

Hao *et al.*, *Science* **371**, 1133–1138 (2021) 12 March 2021

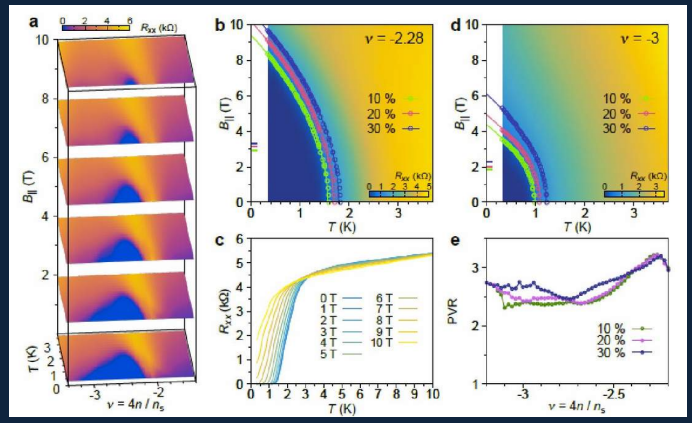


Article

Pauli-limit violation and re-entrant superconductivity in moiré graphene

https://doi.org/10.1038/s41586-021-03685-y
Received: 4 March 2021

Yuan Cao[1,4✉], Jeong Min Park[1,4✉], Kenji Watanabe[2], Takashi Taniguchi[3] & Pablo Jarillo-Herrero[1✉]



Superconductivity in twisted multilayers

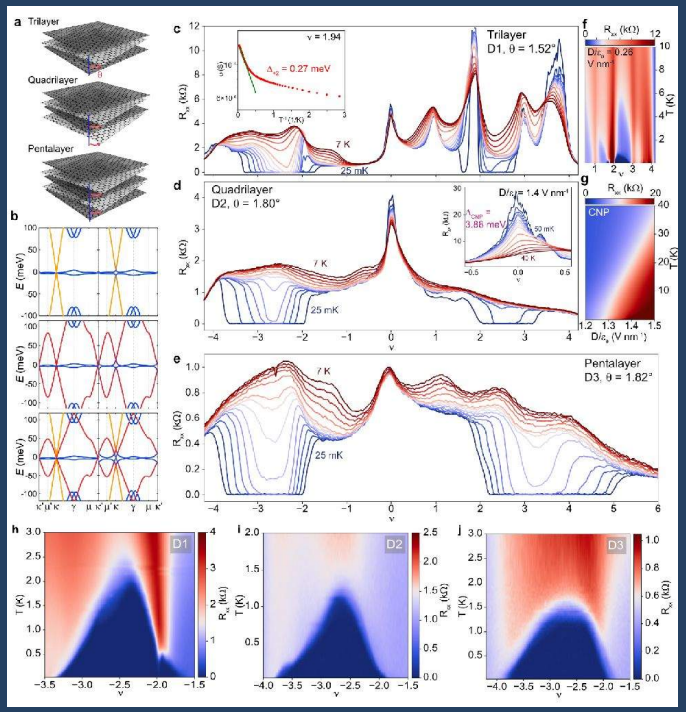
RESEARCH

SUPERCONDUCTIVITY

Promotion of superconductivity in magic-angle graphene multilayers

Yiran Zhang[1,2,3†], Robert Polski[1,2†], Cyprian Lewandowski[2,3], Alex Thomson[2,3,4], Yang Peng[5], Youngjoon Choi[1,2,3], Hyunjin Kim[1,2,3], Kenji Watanabe[6], Takashi Taniguchi[6], Jason Alicea[2,3], Felix von Oppen[7], Gil Refael[2,3], Stevan Nadj-Perge[1,2*]

Zhang *et al.*, *Science* **377**, 1538–1543 (2022) 30 September 2022



nature materials

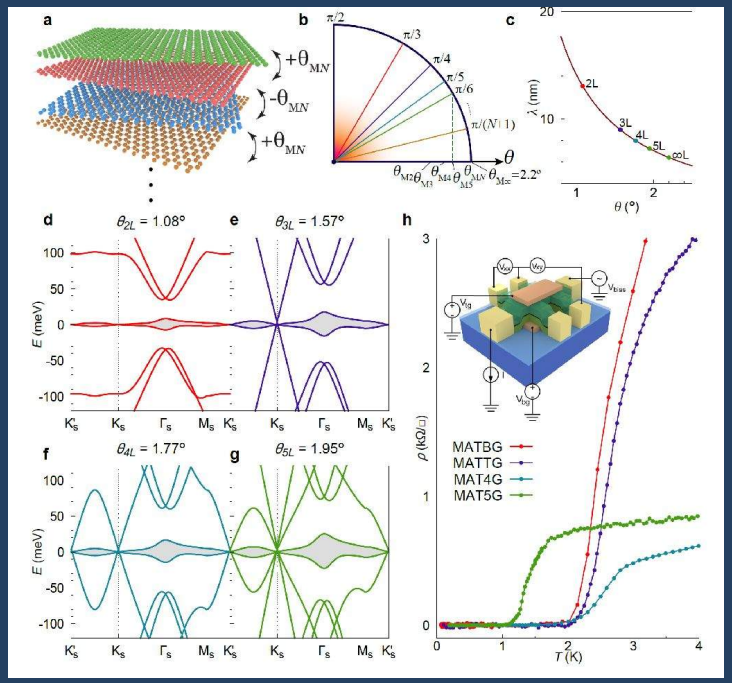
ARTICLES

https://doi.org/10.1038/s41563-022-01287-1

Check for updates

Robust superconductivity in magic-angle multilayer graphene family

Jeong Min Park[1,3], Yuan Cao[1,3], Li-Qiao Xia[1], Shuwen Sun[1], Kenji Watanabe[2], Takashi Taniguchi[2] and Pablo Jarillo-Herrero[1]



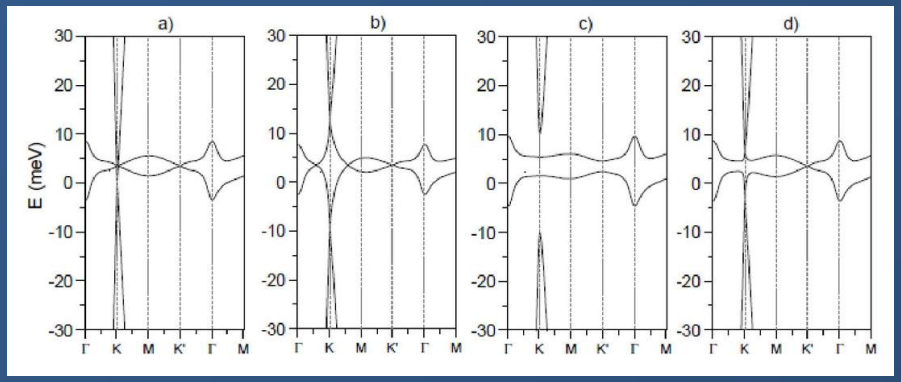
Superconductivity in twisted trilayers: theory

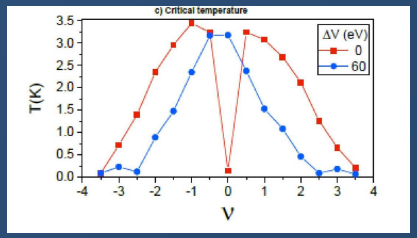
PHYSICAL REVIEW B **104**, L121116 (2021)

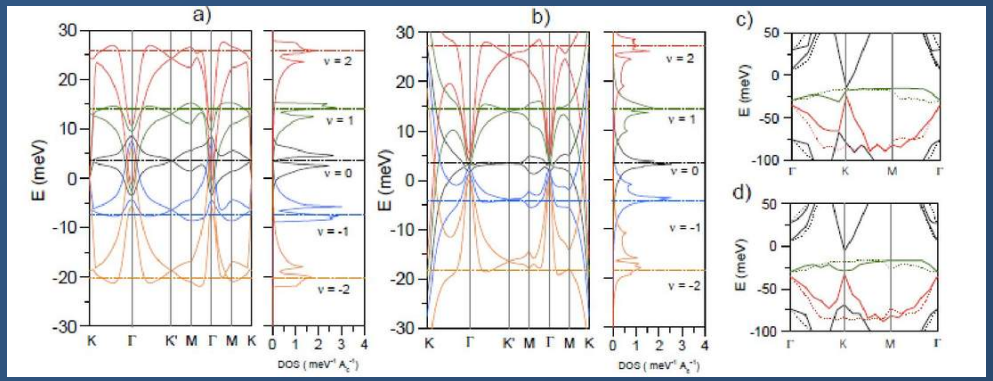
Letter

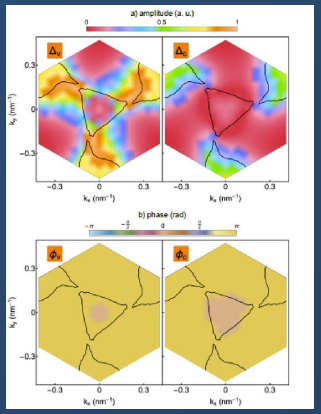
Band structure and superconductivity in twisted trilayer graphene

Võ Tiến Phong,[1] Pierre A. Pantaleón,[2] Tommaso Cea,[2] and Francisco Guinea[2,3]









Superconductivity in graphene without a moiré superlattice

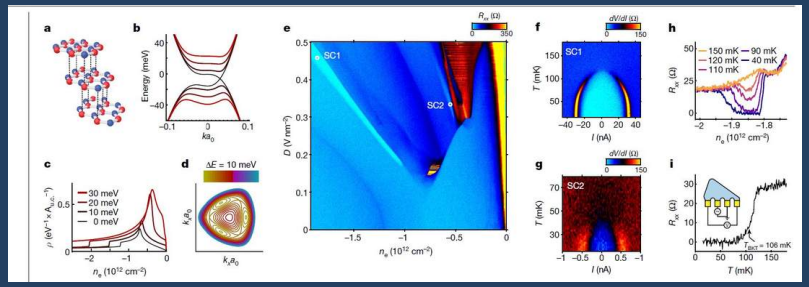
Article

Superconductivity in rhombohedral trilayer graphene

https://doi.org/10.1038/s41586-021-03926-0

Haoxin Zhou[1], Tian Xie[1], Takashi Taniguchi[2], Kenji Watanabe[3] & Andrea F. Young[1]✉

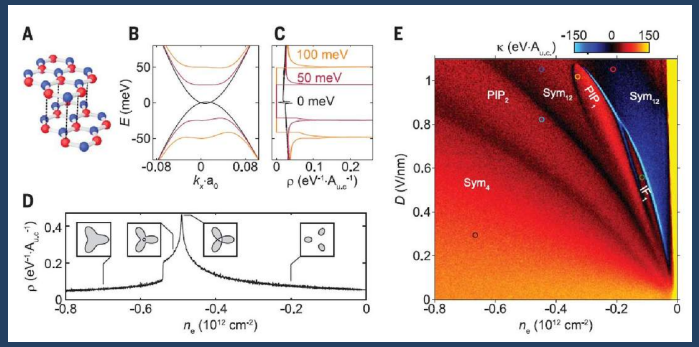
434 | Nature | Vol 598 | 21 October 2021



Isospin magnetism and spin-polarized superconductivity in Bernal bilayer graphene

Haoxin Zhou[1]†, Ludwig Holleis[1], Yu Saito[1], Liam Cohen[1], William Huynh[1], Caitlin L. Patterson[1], Fangyuan Yang[1], Takashi Taniguchi[2], Kenji Watanabe[3], Andrea F. Young[1]*

Zhou *et al.*, *Science* **375**, 774–778 (2022) 18 February 2022



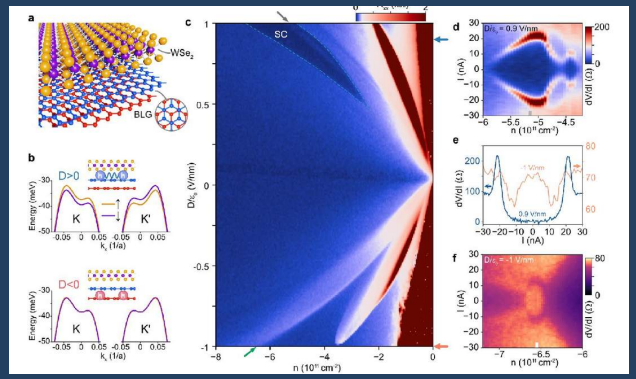
Article

Enhanced superconductivity in spin–orbit proximitized bilayer graphene

https://doi.org/10.1038/s41586-022-05446-x
Received: 5 May 2022

Yiran Zhang[1,2,3], Robert Polski[1,2], Alex Thomson[2,3,4], Étienne Lantagne-Hurtubise[2,3], Cyprian Lewandowski[2,3], Haoxin Zhou[1,2], Kenji Watanabe[5], Takashi Taniguchi[5], Jason Alicea[2,3] & Stevan Nadj-Perge[1,2]✉

268 | Nature | Vol 613 | 12 January 2023

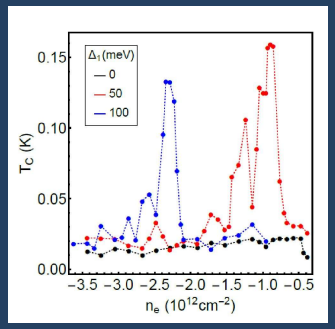


Superconductivity in graphene without a moiré superlattice: theory

PHYSICAL REVIEW B **105**, 075432 (2022)

Superconductivity from repulsive interactions in rhombohedral trilayer graphene: A Kohn-Luttinger-like mechanism

Tommaso Cea and Pierre A. Pantaleón
Instituto Nanociencias, Faraday 9, 28015 Madrid, Spain
Vò Tiến Phong
Department of Physics and Astronomy, University of Pennsylvania, Philadelphia PA 19104, USA
Francisco Guinea



PHYSICAL REVIEW B **107**, L161106 (2023)
Letter
Editors' Suggestion

Superconductivity from electronic interactions and spin-orbit enhancement in bilayer and trilayer graphene

Alejandro Jimeno-Pozo,[1,*] Héctor Sainz-Cruz,[1] Tommaso Cea,[1,2] Pierre A. Pantaleón,[1] and Francisco Guinea[1,3]

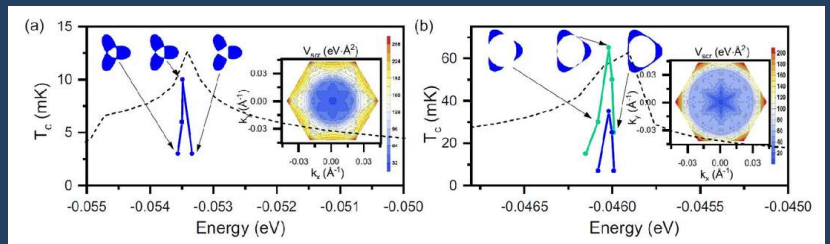


FIG. 2. Superconducting critical temperature due to only the screened long-range Coulomb interaction (blue), and including also the short-range interaction (green), and DOS (a.u., dashed black) versus Fermi energy in (a) BBG with hole doping, near the vHs ($n_e \approx -0.87 \times 10^{12}$ cm^{-2}), we observe a $T_c \approx 10$ mK, and (b) RTG with hole doping, near the vHs ($n_e \approx -0.6 \times 10^{12}$ cm^{-2}), $T_c \approx 33$ mK and it raises to $T_c \approx 65$ mK after including the short-range interaction. The top insets show the shape of the Fermi surfaces, which experience a change in topology at the vHs due to Lifshitz transitions. Right insets: screened Coulomb potential to k_A at the energy for which T_c is maximum.

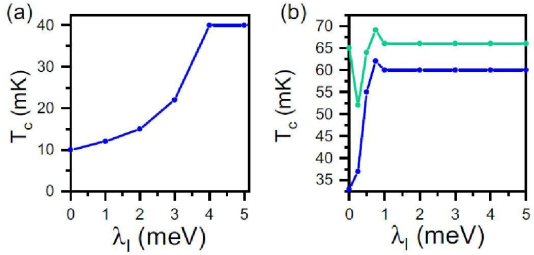
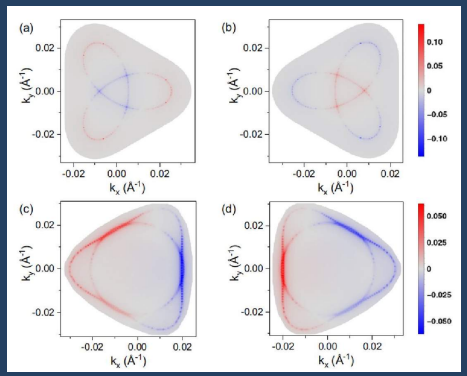
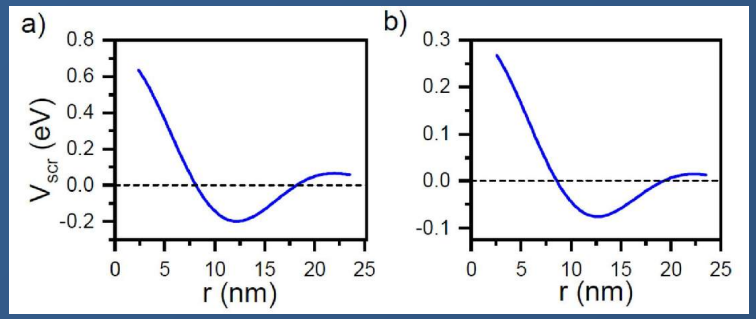
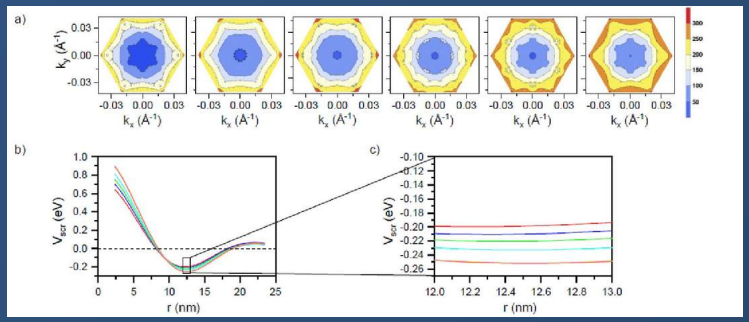


FIG. 3. Ising spin-orbit coupling enhancement of critical temperature in hole-doped (a) BBG, for which T_c augments by a factor of 4 and saturates at $\lambda_I = 4$ meV. (b) RTG, for which T_c due to long-range interactions (blue) augments by a factor of 2 and saturates at $\lambda_I = 1$ meV. In contrast, Ising SOC is detrimental to short-range interactions, so T_c does not increase much when they are included (green).



Superconductivity graphene without a moiré superlattice:effective attraction





Effect of spin-orbit coupling

PHYSICAL REVIEW B **88**, 054515 (2013)

Interactions and superconductivity in heavily doped MoS_2

R. Roldán,[1] E. Cappelluti,[1,2] and F. Guinea[1]

RESEARCH ARTICLE | AUGUST 13 2013

Superconductivity from repulsive interaction FREE

Saurabh Maiti; Andrey V. Chubukov

AIP Conf. Proc. 1550, 3–73 (2013)

https://doi.org/10.1063/1.4818400

edral trilayer

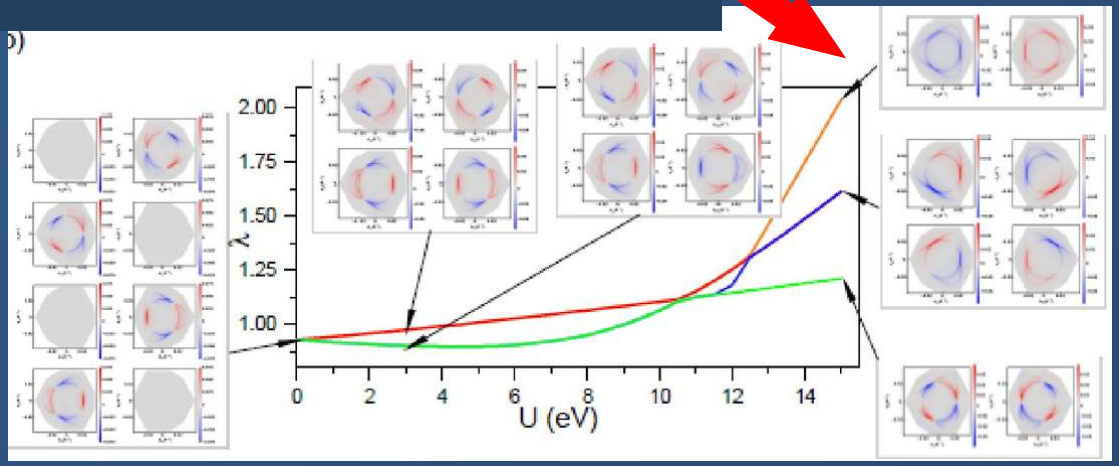
PHYSICAL REVIEW B **107**, L041111 (2023)

Letter

Superconductivity induced by the intervalley Coulomb scattering in a few layers of gr

Tommaso Cea

real space



Order parameter and intervalley interactions

$$V_{scr}(\vec{q}) = \frac{V_C(\vec{q})}{1 - V_C(\vec{q})\chi(\vec{q})} \approx \frac{1}{|\chi(\vec{q})|}$$

SOC, due to flavor polarization, lowers screening, and increases both repulsion and attraction

PHYSICAL REVIEW B **108**, 045404 (2023)

Charge fluctuations, phonons, and superconductivity in multilayer graphene

Ziyan Li,[1,2] Xueheng Kuang,[1,2] Alejandro Jimeno-Pozo,[2] Héctor Sainz-Cruz,[2] Zhen Zhan,[2,1,*] Shengjun Yuan,[1,3] and Francisco Guinea[2,4]

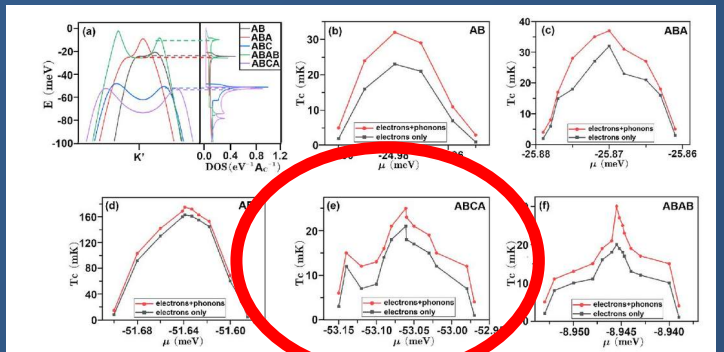


FIG. 4. (a) Band structures and DOS near the CNP in [illegible] graphene [illegible] Superconducting critical temperatures versus Fermi energy near the VHS in five different multilayer graphene stacks, due to electron interactions only or taking into account also the effects of electron-acoustic phonon coupling.

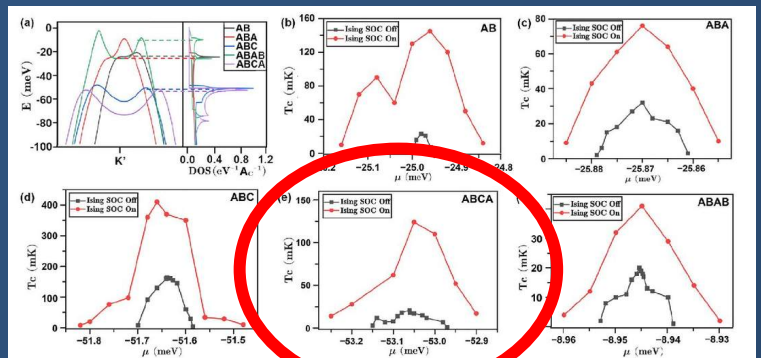


FIG. 5. (a) Bands and DOS near VHS in multilayer [illegible] with displacement field $\Delta_1 = 50$ meV. (b)–(f) Critical temperature of multilayer graphene with and without Ising SOC, with Fermi energy near VHS.

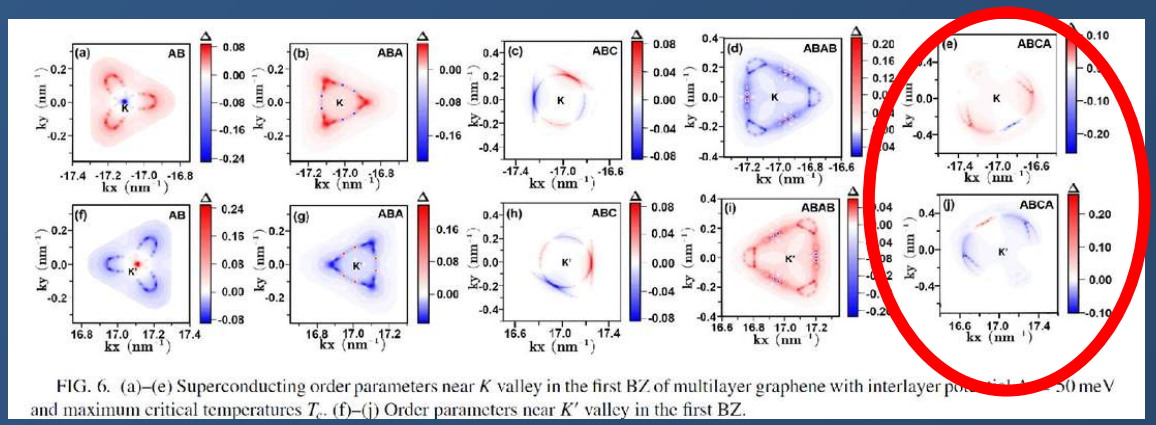


FIG. 6. (a)–(e) Superconducting order parameters near K valley in the first BZ of multilayer graphene with interlayer potential [illegible] 50 meV and maximum critical temperatures T_c. (f)–(j) Order parameters near K' valley in the first BZ.

Quarter metal phase

- Lack of Cooper divergence, 1st order transition?
- Does the symmetries change in the superconducting phase?
- Role of trigonal distortion.

Tuning repulsive interactions and superconductivity

nature physics

Article

https://doi.org/10.1038/s41567-026-03243-1

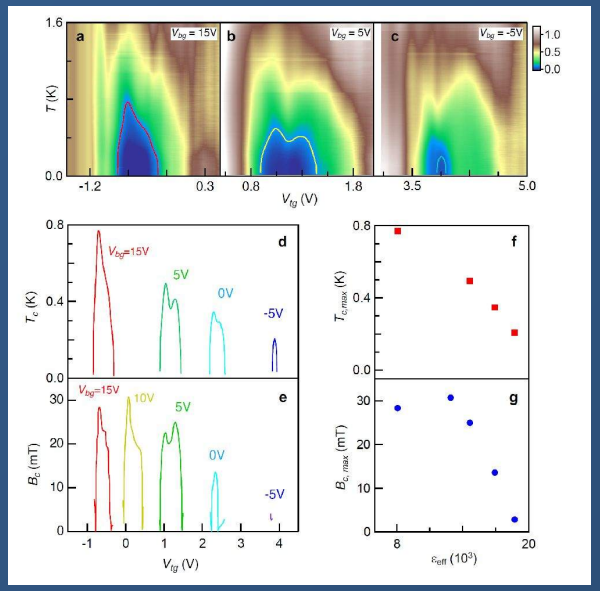
Double-edged role of interactions in superconducting twisted bilayer graphene

Received: 22 December 2024

Accepted: 5 March 2026

Published online: 07 April 2026

Xueshi Gao[1], Alejandro Jimeno-Pozo[2], Pierre A. Pantaleon[2], Aatmaj Rajesh[1], Emilio Codecido[1,3], Daria L. Sharifi[1], Zheneng Zhang[1], Youwei Liu[1], Kenji Watanabe[4], Takashi Taniguchi[5], Marc W. Bockrath[1], Francisco Guinea[2,6] & Chun Ning Lau[1]

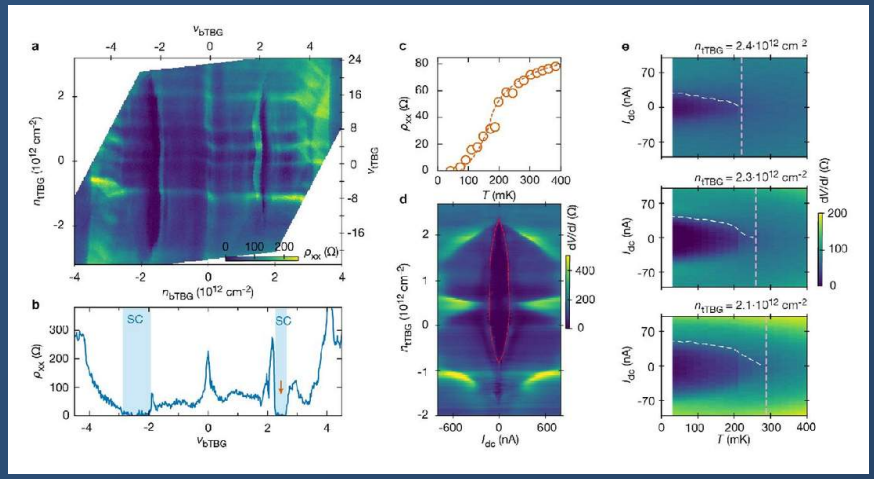


PHYSICAL REVIEW X 16, 031040 (2026)

Featured in Physics

Coulomb Screening of Superconductivity in Magic-Angle Graphene

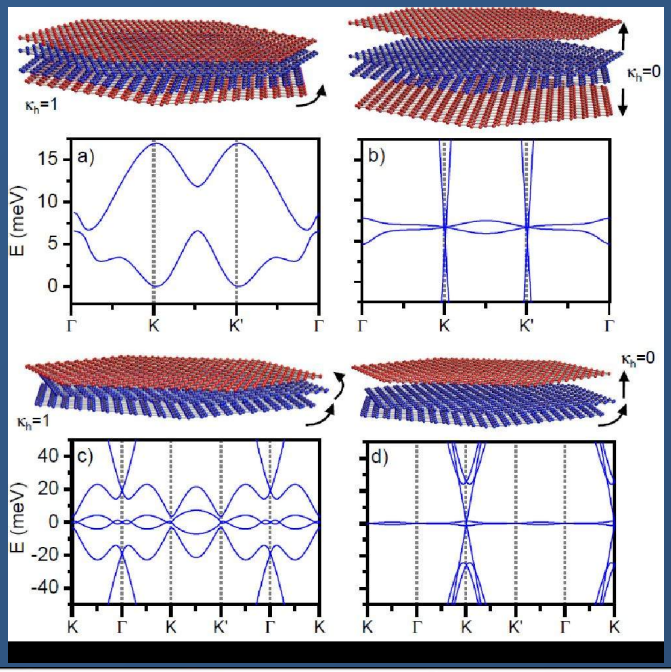
Julien Barrier[1,2,*] Liangtao Peng[3] Shuigang Xu[2] Christophe De Beule[4,5] V. I. Fal'ko[1,2,6] K. Watanabe[7] T. Taniguchi[7] A. K. Geim,[1,2,§] Shaffique Adam[3,8,‡] and Alexey I. Berdyugin[8,9,1,†]



Twisted double bilayer and helical trilayer graphene

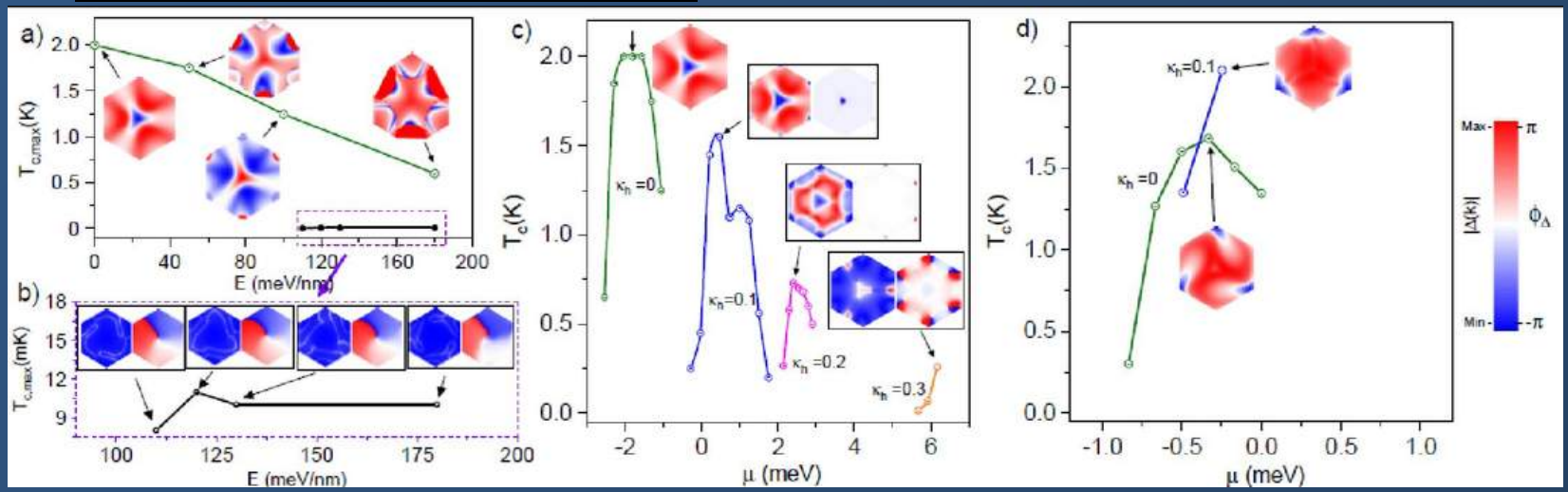
Interlayer Coupling Driven Superconductivity in Twisted Double Bilayer Graphene

Min Long,[1,2,*] Alejandro Jimeno-Pozo,[3,*] Héctor Sainz-Cruz,[3] Pierre A. Pantaleón,[1,†] and Francisco Guinea[1,4,5]



arXiv:2401.09667, PNAS **121** (32) e2405259121 (2024)

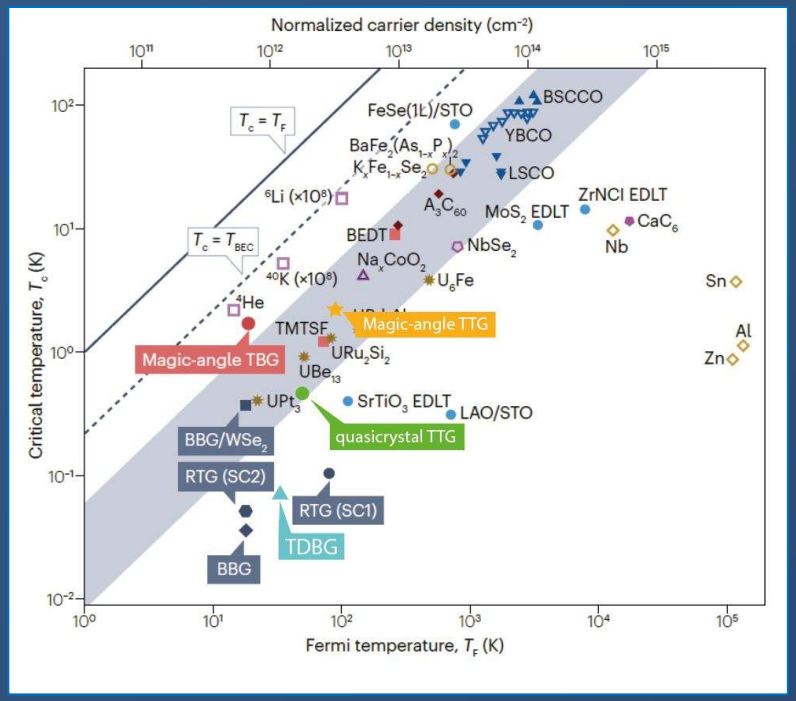
	ee+ph+G	ee+G	ee+ph	ee
TBG				
TDBG				
hTTG			??	??

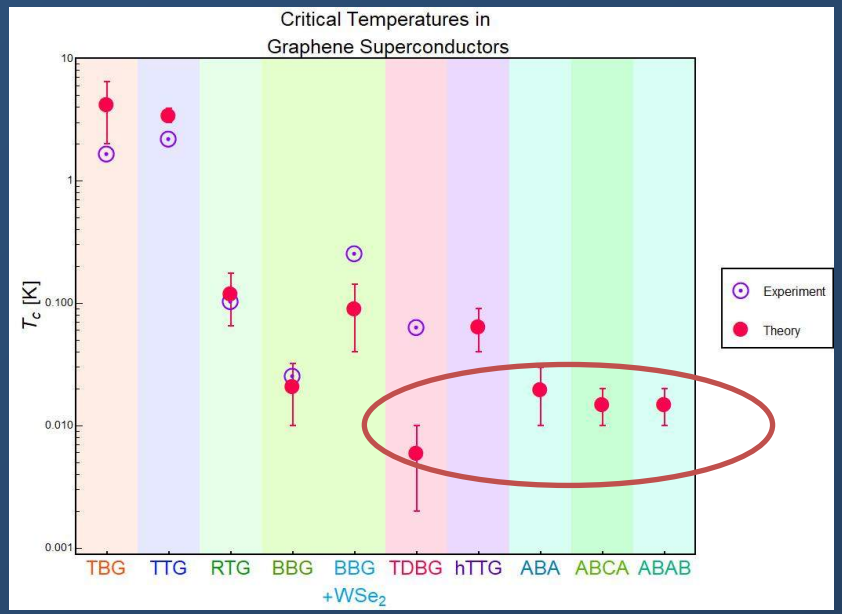


Long range electron-electron interactions and superconductivity in graphene stacks

- Strongest interaction in twisted bilayer graphene
- Few adjustable parameters, $\epsilon \approx 6 - 10$
- Describes well general trends
- Broken symmetry phases not included

Electronic bands								Coulomb potential		Deformation potential and elastic constants		
2.46	5.253	0.4	0.32	0.044	0.05	0.797	0.0975	40	10	20	3.25	9.44

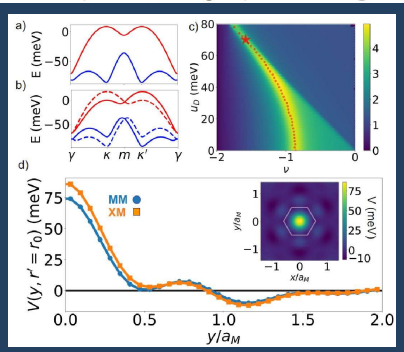




Other recent RPA+KL calculations of superconductivity

Topological superconductivity from repulsive interactions in twisted WSe_2

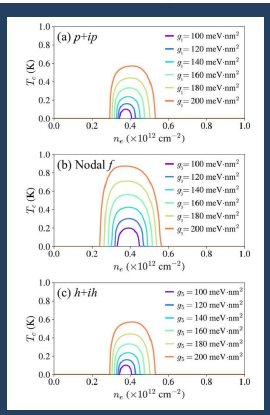
Daniele Guerci,[1,*] Daniel Kaplan,[2,†] Julian Ingham,[3,1] J. H. Pixley,[2,1] and Andrew Millis[3,1]



arXiv:2408.16075

Intravalley spin-polarized superconductivity in rhombohedral tetralayer graphene

Yang-Zhi Chou,[1,*] Jihang Zhu,[1,†] and Sankar Das Sarma[1,2]



Phys. Rev. B **111**,174523 (2025)

nature communications

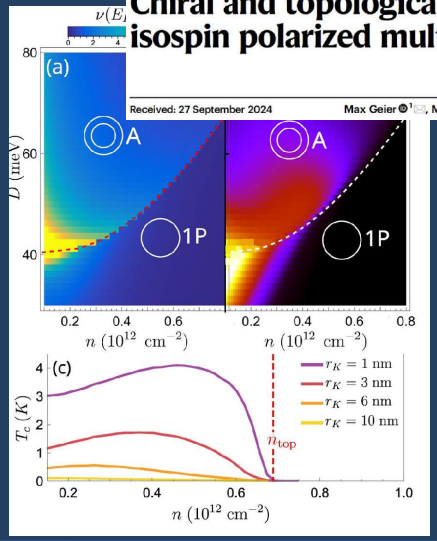
Article

https://doi.org/10.1038/s41467-025-66902-6

Chiral and topological superconductivity in isospin polarized multilayer graphene

Received: 27 September 2024

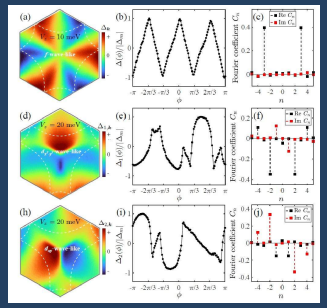
Max Geier[1], Margarita Davydova[1,2] & Liang Fu[1]



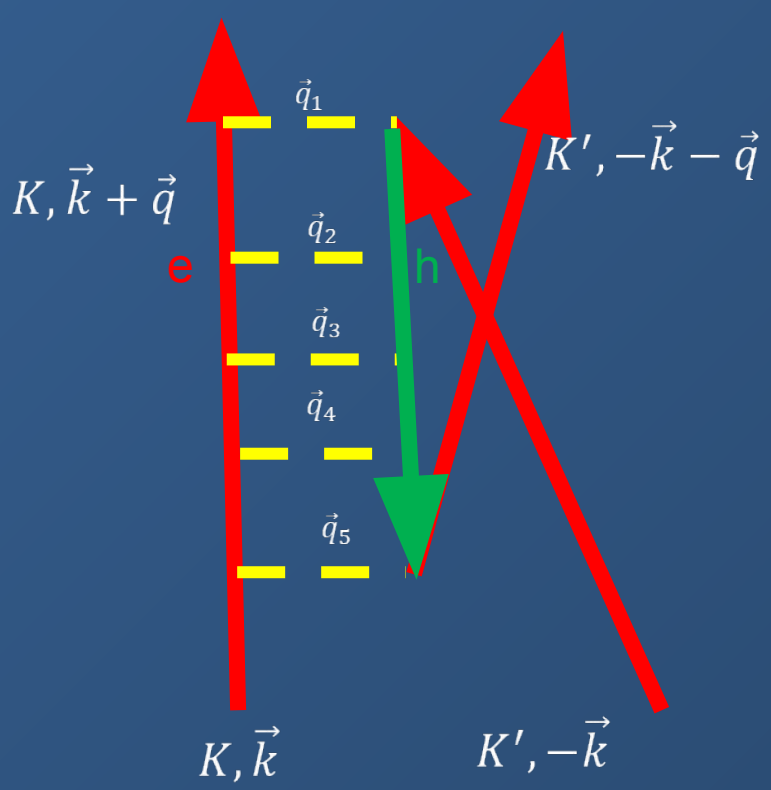
PHYSICAL REVIEW LETTERS **135,** 246002 (2025)

Topological Chiral Superconductivity Mediated by Intervalley Antiferromagnetic Fluctuations in Twisted Bilayer WSe_2

Wei Qin,[1,*,†] Wen-Xuan Qiu,[2,*] and Fengcheng Wu[2,‡]

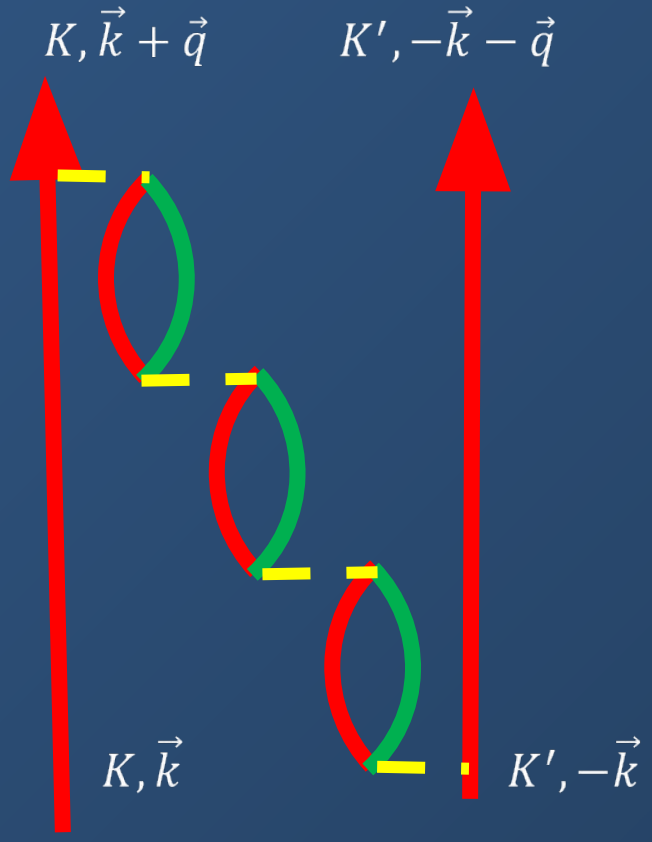


Soft spin and valley modes, broken symmetries



$$V_{\vec{G},\vec{G}'}(\vec{q},\omega) = V^0_{\vec{G},\vec{G}'}(\vec{q},\omega)\left(1 - \Pi_{\vec{G},\vec{G}'}(\vec{q},\omega)\right)^{-1}$$

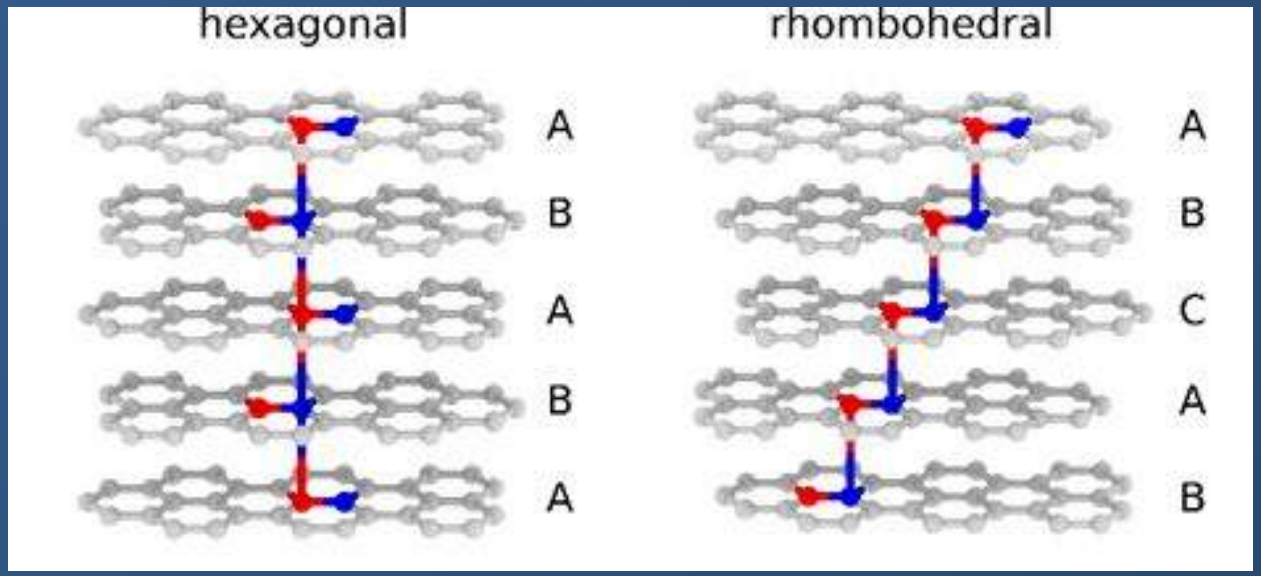
Spin, valley, …, waves



$$V_{\vec{G},\vec{G}'}(\vec{q},\omega) = V^0_{\vec{G},\vec{G}'}(\vec{q},\omega)\left(1 + \Pi_{\vec{G},\vec{G}'}(\vec{q},\omega)\right)^{-1}$$

Charge fluctuations

Three dimensional rhombohedral graphite

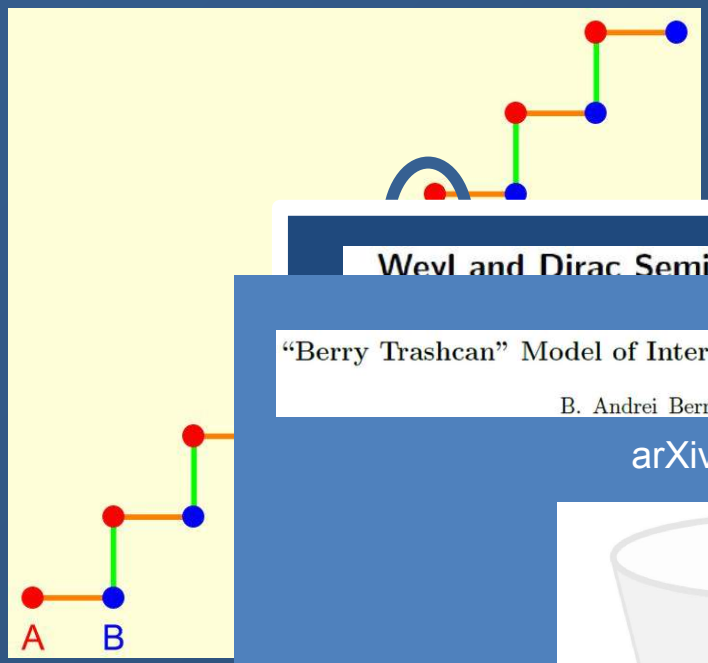


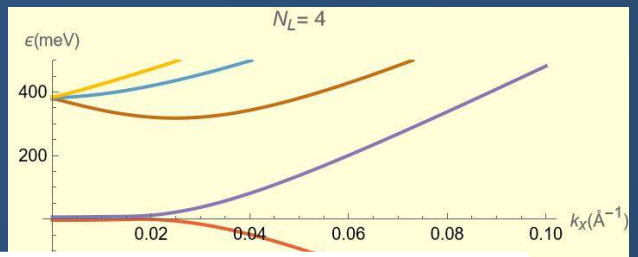
Bernal graphite ABABAB

Rhombohedral graphite ABCABC

About 10% of natural graphite shows rhombohedral stacking (M. Dresselhaus, private communication)

Flat bands in thick rhombohedral multilayers





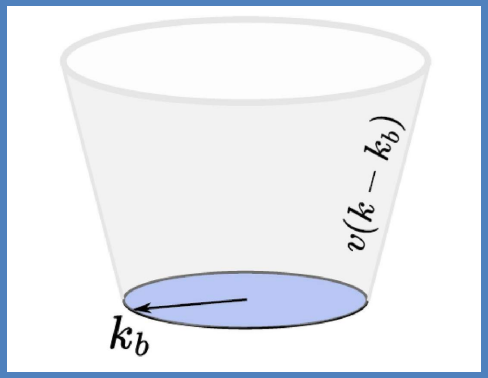
Weyl and Dirac Semimetals in Three Dimensional Solids*

University, Baltimore,

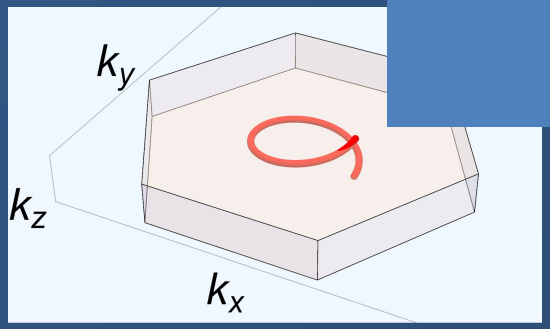
"Berry Trashcan" Model of Interacting Electrons in Rhombohedral Graphene

B. Andrei Bernevig[1,2,3] and Yves H. Kwan[4]

arXiv:2503.09692

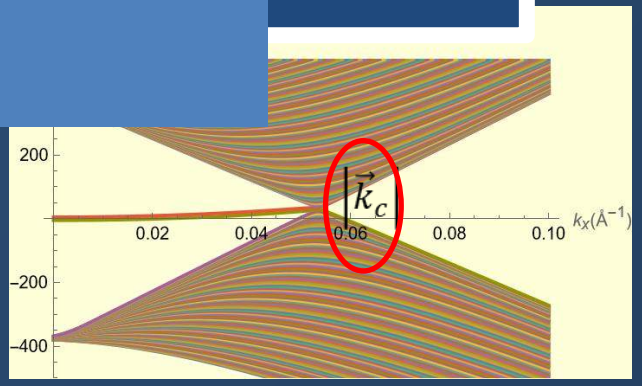


Su-Sc



$$v_F$$

$$\rho_c = \frac{\left|\vec{k}_c\right|^2}{4\pi} \approx 10^{13}\,\mathrm{cm}^{-2}$$



Surface elec

- Metallic bulk:

Finite density of state
the gate is screened v
$l_{TF} \sim \left(e^2 N(E_F)\right)^{-1}$.

- Semiconducting bu

The potential induced
(valence) band down
region and screen the

ISSN 0021-3640, JETP Letters, 2011, Vol. 94, No. 3, pp. 233–239. © Pleiades Publishing, Inc., 2011.

Flat Bands in Topological Media¶

T. T. Heikkilä[a], N. B. Kopnin[a, b], and G. E. Volovik[a, b]

[a] Low Temperature Laboratory, Aalto University, School of Science and Technology, P.O. Box 15100, FI-00076 AALTO, Finland

[b] Landau Institute for Theoretical Physics, Russian Academy of Sciences, Moscow, 119334 Russia

e-mail: tero.heikkila@tkk.fi, kopnin@boojum.hut.fi, volovik@boojum.hut.fi

Received June 22, 2011

Topological media are systems whose properties are protected by topology and thus are robust to deformations of the system. In topological insulators and superconductors the bulk-surface and bulk-vortex correspondence gives rise to the gapless Weyl, Dirac or Majorana fermions on the surface of the system and inside vortex cores. Here we show that in gapless topological media, the bulk-surface and bulk-vortex correspondence is more effective: it produces topologically protected gapless fermions without dispersion—the flat band. Fermion zero modes forming the flat band are localized on the surface of topological media with protected nodal lines [A. P. Schnyder and S. Ryu, Phys. Rev. B **84**, 060504(R) (2011); T. T. Heikkilä and G. E. Volovik, JETP Lett. **93**, 59 (2011)] and in the vortex core in systems with topologically protected Fermi points (Weyl points) [G. E. Volovik, JETP Lett. **93**, 66 (2011)]. Flat band has an extremely singular density of states, and we show that this property may give rise in particular to surface superconductivity which could exist even at room temperature.

DOI: 10.1134/S0021364011150045

- Rhombohedral graphene:

Vanishing density of states density of states at the Fermi level, but zero gap.

There is a flat band at the surface, even in the absence of a gate. The band is at the neutrality point (nodal system, drumhead band).

Superconductivity in untwisted tetralayers

Signatures of chiral superconductivity in rhombohedral graphene

https://doi.org/10.1038/s41586-025-09169-7
Received: 1 September 2024
Accepted: 16 May 2025
Published online: 22 May 2025

Tonghang Han[1,6], Zhengguang Lu[1,2,6], Zach Hadjri[1,6], Lihan Shi[1], Zhenghan Wu[1], Wei Xu[1], Yuxuan Yao[1], Armel A. Cotten[3], Omid Sharifi Sedeh[3], Henok Weldeyesus[3], Jixiang Yang[1], Junseok Seo[1], Shenyong Ye[1], Muyang Zhou[1], Haoyang Liu[2], Gang Shi[2], Zhenqi Hua[2], Kenji Watanabe[4], Takashi Taniguchi[5], Peng Xiong[2], Dominik M. Zumbühl[3], Liang Fu[1] & Long Ju[1]✉

Nature **643**, 654 (2025)

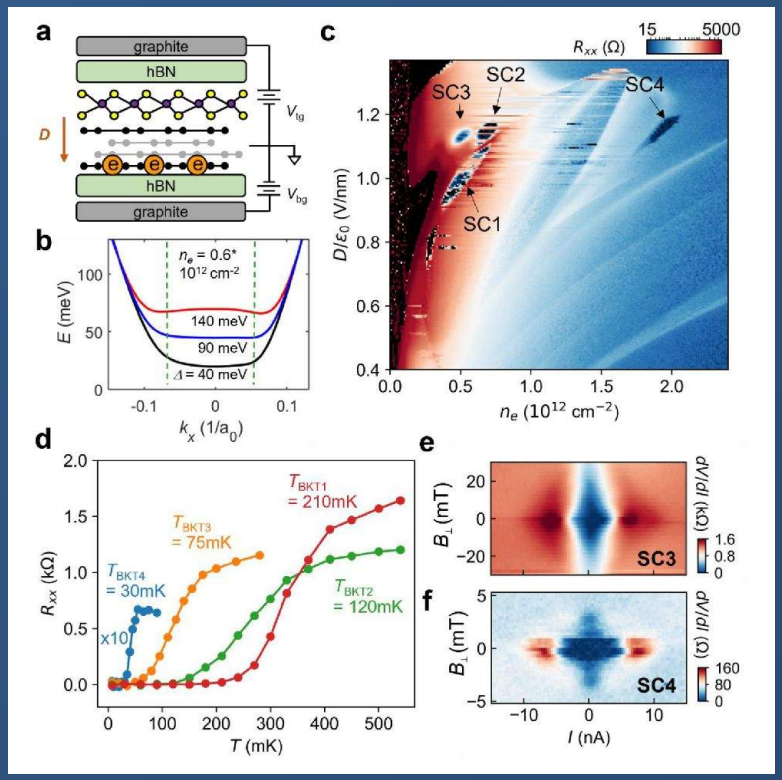
4 layers

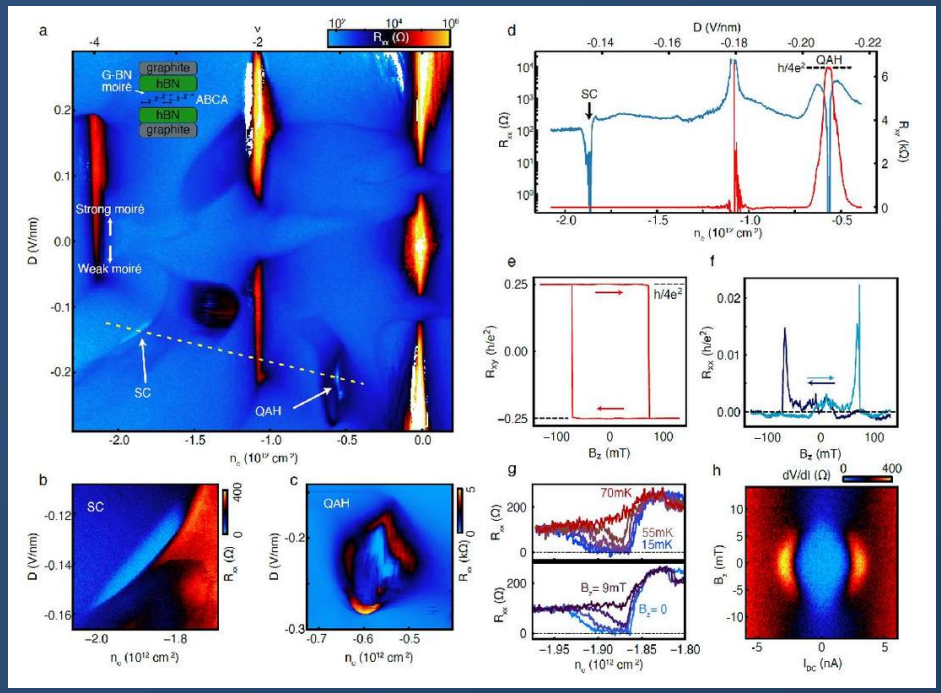
Superconductivity and quantized anomalous Hall effect in rhombohedral graphene

https://doi.org/10.1038/s41586-025-08621-y
Received: 22 August 2024
Accepted: 9 January 2025

Youngjoon Choi[1,4], Ysun Choi[1,4], Marco Valentini[1,4], Caitlin L. Patterson[1], Ludwig F. W. Holleis[1], Owen I. Sheekey[1], Hari Stoyanov[1], Xiang Cheng[1], Takashi Taniguchi[2], Kenji Watanabe[3] & Andrea F. Young[1]✉

Nature **639**, 342 (2025)





More experiments

nature physics

Article

https://doi.org/10.1038/s41567-026-03277-5

Superconductivity from dual-surface carriers in rhombohedral graphene

Received: 26 October 2025

Accepted: 30 March 2026

Manish Kumar[1,9], Derek Waleffe[1,9], Anna Okounkova[1,9], Raveel Tejani[2,3], Võ Tiến Phong[4,5], Kenji Watanabe[6], Takashi Taniguchi[7], Cyprian Lewandowski[4,5], Joshua Folk[2,3] ✉ & Matthew Yankowitz[1,8] ✉

6 layers

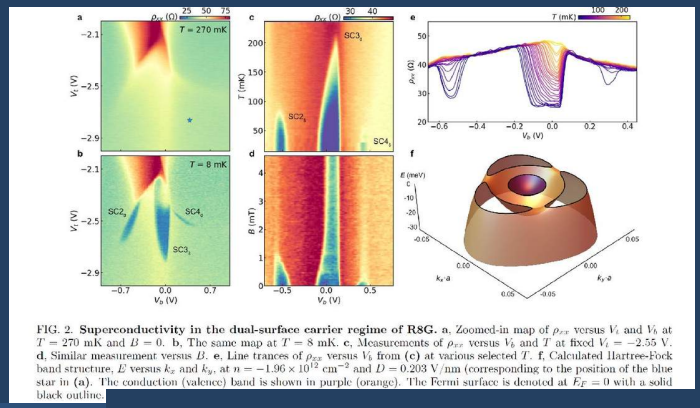
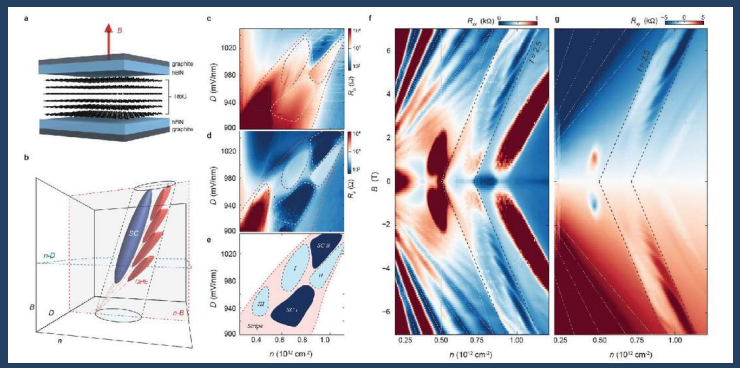


FIG. 2. **Superconductivity in the dual-surface carrier regime of R8G.** a, Zoomed-in map of ρ_{xx} versus V_t and V_b at $T = 270$ mK and $B = 0$. b, The same map at $T = 8$ mK. c, Measurements of ρ_{xx} versus V_b and T at fixed $V_t = -2.55$ V. d, Similar measurement versus B. e, Line traces of ρ_{xx} versus V_b from (c) at various selected T. f, Calculated Hartree-Fock band structure, E versus k_x and k_y, at $n = -1.96 \times 10^{12}$ cm^{-2} and $D = 0.203$ V/nm (corresponding to the position of the blue star in (a). The conduction (valence) band is shown in purple (orange). The Fermi surface is denoted at $E_F = 0$ with a solid black outline.

A Hierarchy of Topological and Superconducting States in Rhombohedral Hexalayer Graphene

Ron Q. Nguyen[1,*] Hai-Tian Wu[1,*] Erin Morissette[1,*] Naiyuan J. Zhang[1,*] Peiyu Qin[1], K. Watanabe[2], T. Taniguchi[3], Aaron W. Hui[1], D. E. Feldman[1,5], and J.I.A. Li[1,4†]

arXiv:2507.22026



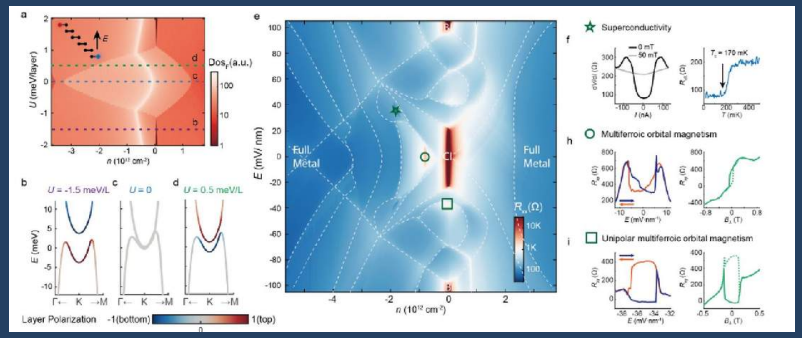
6 layers

Superconductivity and Ferroelectric Orbital Magnetism in Semimetallic Rhombohedral Hexalayer Graphene

Jinghao Deng[1#], Jiabin Xie[1#], Hongyuan Li[1#], Takashi Taniguchi[2], Kenji Watanabe[3], Jie Shan[4,5], Kin Fai Mak[1,5], Xiaomeng Liu[1]*

arXiv:2508.15909

6 layers



More experiments

nature materials

Article

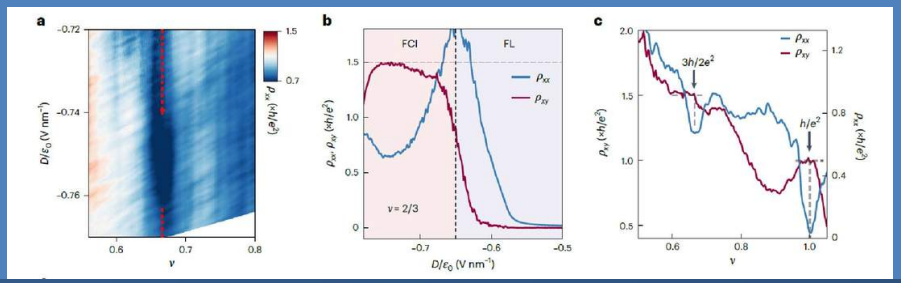
https://doi.org/10.1038/s41563-025-02225-7

Tunable fractional Chern insulators in rhombohedral graphene superlattices

Received: 16 January 2025
Accepted: 25 March 2025

Jian Xie[1], Zihao Huo[1], Xin Lu[2], Zuo Feng[3], Zaizhe Zhang[1], Wenxuan Wang[1], Qiu Yang[1], Kenji Watanabe[4], Takashi Taniguchi[5], Kaihui Liu[3], Zhida Song[1,2], X. C. Xie[1,2,6], Jianpeng Liu[2,6] & Xiaobo Lu[1]

6 layers



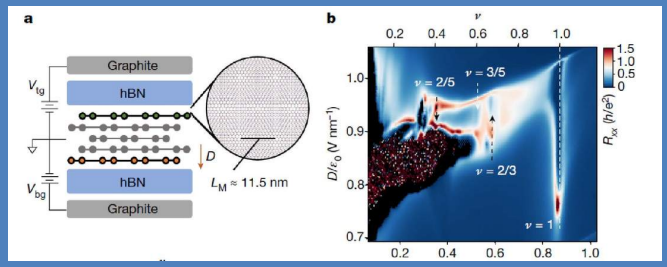
Article

Fractional quantum anomalous Hall effect in multilayer graphene

https://doi.org/10.1038/s41586-023-07010-7
Received: 1 October 2023

Zhengguang Lu[1,4], Tonghang Han[1,4], Yuxuan Yao[1,4], Aidan P. Reddy[1], Jixiang Yang[1], Junseok Seo[1], Kenji Watanabe[2], Takashi Taniguchi[3], Liang Fu[1] & Long Ju[1]

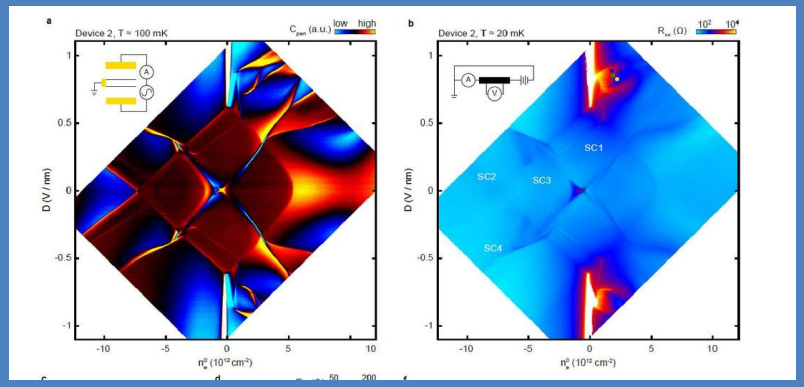
5 layers



Flat band surface state superconductivity in thick rhombohedral graphene

Yi Guo,[1] Owen I. Sheekey,[1] Trevor Arp,[1] Kryštof Kolář,[2] Thibault Charpentier,[1] Ludwig Holleis,[1] Ben Foutty,[1] Aidan Keough,[1] Maya Kang-Chou,[1] Martin E. Huber,[3] Takashi Taniguchi,[4] Kenji Watanabe,[5] Cyprian Lewandowski,[6,7] and Andrea F. Young[1,*]

arXiv:2511.17423

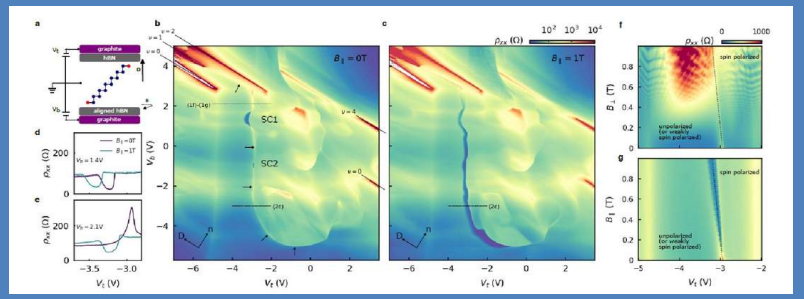


13 layers

Pervasive spin-triplet superconductivity in rhombohedral graphene

Manish Kumar[1*], Derek Waleffe[1*], Anna Okounkova[1*], Raveel Tejani[2,3], Kenji Watanabe[6], Takashi Taniguchi[7], Étienne Lantagne-Hurtubise[8], Joshua Folk[2,3†], and Matthew Yankowitz[1,9†]

arXiv:2511.16578



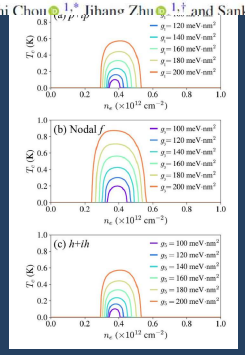
7 layers

Some calculations in a fully polarized tetralayer

PHYSICAL REVIEW B **111**, 174523 (2025)

Intravalley spin-polarized superconductivity in rhombohedral tetralayer graphene

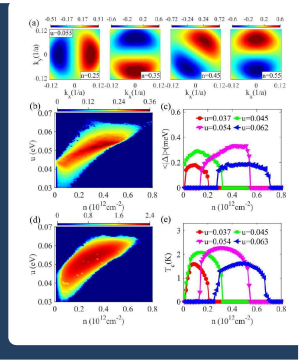
Yang-Zhi Chou, Jihang Zhu, and Sankar Das Sarma



Chiral finite-momentum superconductivity in the tetralayer graphene

Qiong Qin[1] and Congjun Wu[1,2,3,4,*]

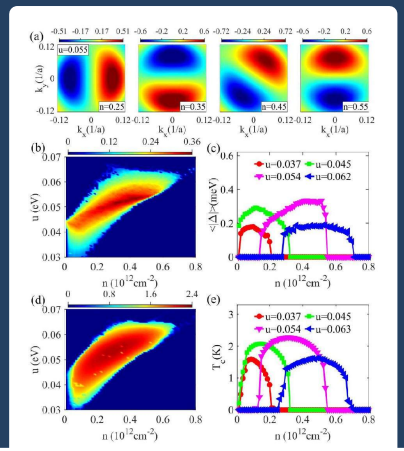
arXiv:2412.07145, Chin. Phys. Lett. **43**, 030708 (2026)



Quarter Metal Superconductivity

Chiho Yoon,[1] Tianyi Xu,[1] Yafis Barlas,[2] and Fan Zhang[1]

Phys. Rev. Lett. 136, 026603 (2026)



nature communications

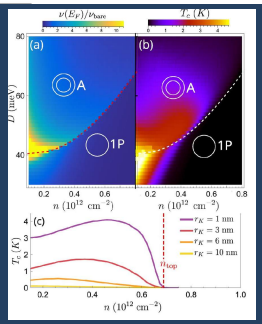
Article

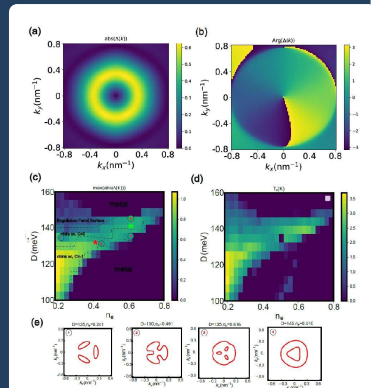
https://doi.org/10.1038/s41467-025-66902-6

Chiral and topological superconductivity in isospin polarized multilayer graphene

Received: 27 September 2024

Max Geier[1], Margarita Davydova[1,2] & Liang Fu[1]





PHYSICAL REVIEW B **112**, L020506 (2025)

Letter | Editors' Suggestion

Topological incommensurate Fulde-Ferrell-Larkin-Ovchinnikov superconductor and Bogoliubov Fermi surface in rhombohedral tetralayer graphene

Hui Yang and Ya-Hui Zhang

PHYSICAL REVIEW LETTERS **135,** 136503 (2025)

Band Renormalization, Quarter Metals, and Chiral Superconductivity in Rhombohedral Tetralayer Graphene

Guillermo Parra-Martínez,[1,*] Alejandro Jimeno-Pozo,[1,*] Võ Tiến Phong,[2,3] Héctor Sainz-Cruz,[1] Daniel Kaplan,[4] Peleg Emanuel,[5] Yuval Oreg,[5] Pierre A. Pantaleón,[1,†] José Ángel Silva-Guillén,[1,‡] and Francisco Guinea[1,6]

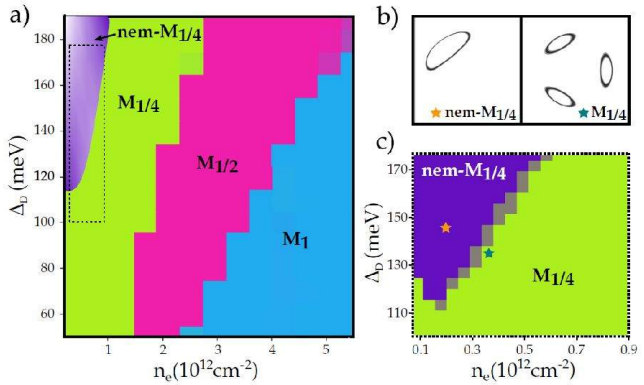


Figure 1. **Hartree-Fock phase diagram.** (a) Self-consistently calculated HF phase diagram, showing $M_{1/4}$, $M_{1/2}$ and M_1 phases as a function of the external displacement field (Δ_D) and electronic density (n_e). The purple region at low densities and high displacement fields highlights schematically where the nem-$M_{1/4}$ is expected to emerge. In (c), we show the calculated phase boundary between $M_{1/4}$ and nem-$M_{1/4}$ in the region indicated by a dashed rectangle in (a). (b) Representative Fermi surfaces at the same point in parameter space indicated by the yellow and blue stars in (c) solutions with and without $\mathcal{C}_3$ symmetry breaking.

- A variety of polarized phases
- Multiple Lifchitz transitions.
- Significant trigonal warping

The HF density of states shows an unphysical dip at the Fermi energy.
The bands are not suited for the calculation of superconductivity.

Superconductivity. Critical temperature

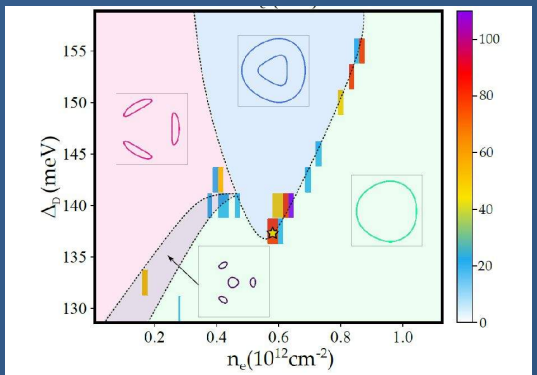


Figure 3. **Superconductivity critical temperature.** Superconducting critical temperature, T_c, as a function of displacement and electron filling in the $M_{1/4}$ phase. The colored regions indicate different Fermi surface shapes. Black dashed lines mark Lifshitz transitions, between different shapes of the fermi surfaces (see section IV SM [47]). A representative Fermi surface is displayed within each region. The yellow star indicates the parameters used for the calculation of the superconducting order parameter (OP) shown in Fig. 4(a-b).

- Calculations carried out using the RPA screened interaction.
- Trigonal warping suppresses the Cooper instability.
- Narrow slice in phase space where superconductivity appears.

Superconductivity. Order parameter

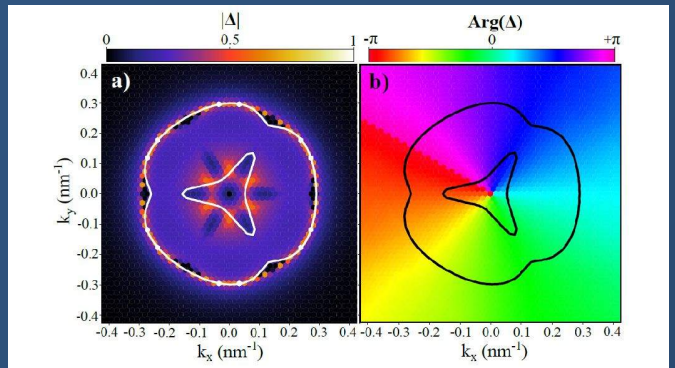


Figure 4. **Superconducting order parameter**. Order parameter of the leading eigenvalue in the screened Hartree-Fock superconductivity calculations. (a) Normalized magnitude of the order parameters and (b) its corresponding phase. The Fermi surface is indicated by solid white and black lines in each panel, respectively. Calculations were made at values $\Delta_D = 137.5$ meV and $n_e = 6.01 \times 10^{11} cm^{-2}$ with $T_c = 80$ mK, marked in Fig. 3 as a yellow star.

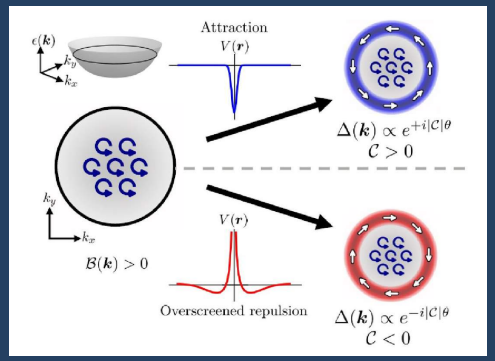
- p-wave superconductivity
- No degeneracy between p_+ and p_- .
- The gap in not pinned to the Fermi surface
- Gapless superconductivity, due to the par breaking effects oftrigonal warping. Similar to s-wave superconductors with magnetic impurities.

Other works on quarter metal superconductivity

How pairing mechanism dictates topology in valley-polarized superconductors with Berry curvature

Julian May-Mann,* Tobias Helbig, and Trithep Devakul†

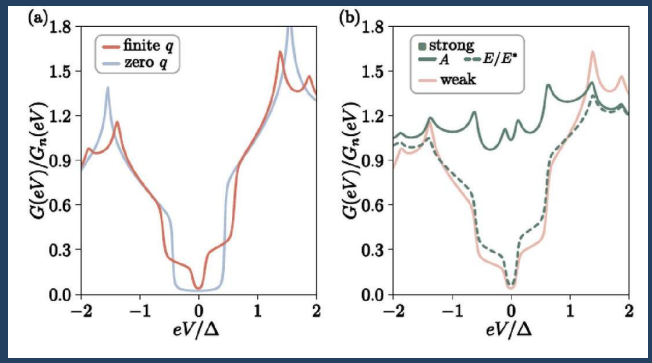
arXiv.2503.05697



Probing superconductivity with tunneling spectroscopy in rhombohedral graphene

Denis Sedov[1] and Mathias S. Scheurer[1]

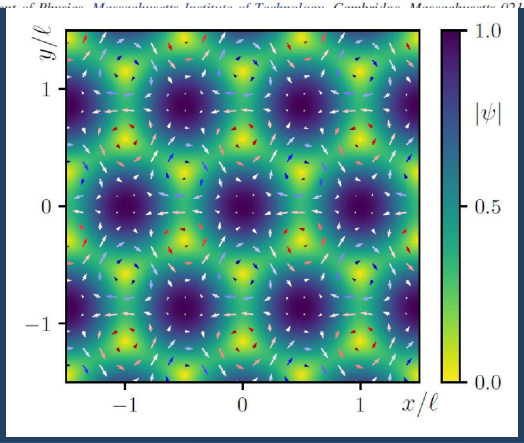
arXiv.2503.12650



PHYSICAL REVIEW LETTERS 135, 116001 (2025)

Spontaneous Vortex-Antivortex Lattice and Majorana Fermions in Rhombohedral Graphene

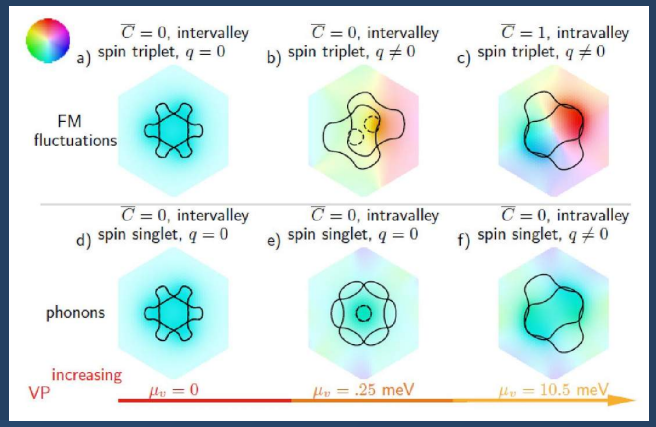
Filippo Gaggioli,* Daniele Guerci,† and Liang Fu‡



Finite-momentum pairing and superlattice superconductivity in valley-imbalanced rhombohedral graphene

Maine Christos,[1] Pietro M. Bonetti,[1] and Mathias S. Scheurer[2]

arXiv.2503.15471



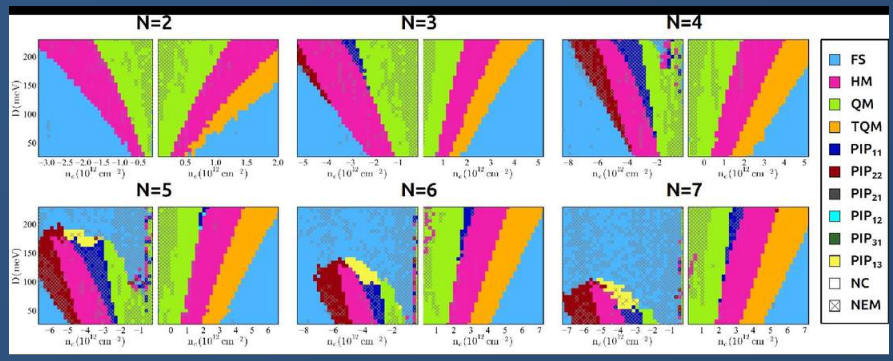
Phase diagrams of rhombohedral multilayers

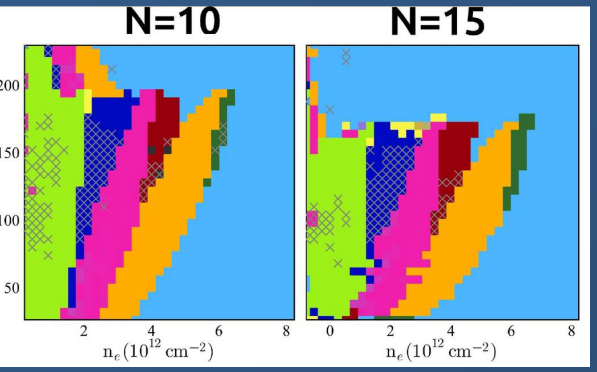
RESEARCH ARTICLE

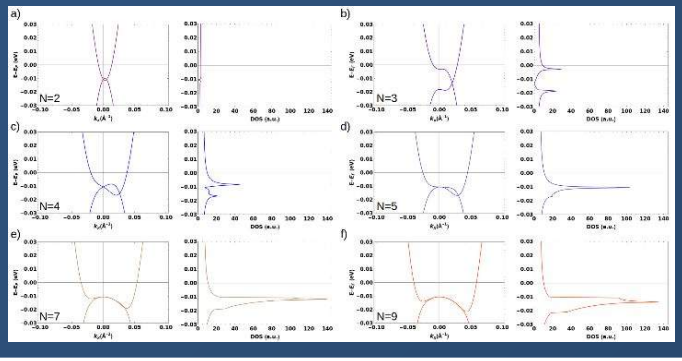
ADVANCED MATERIALS
www.advmat.de

Nematic and Partially Polarized Phases in Rhombohedral Graphene with Varying Number of Layers: An Extensive Hartree–Fock Study

Guillermo Parra-Martínez, Alejandro Jimeno-Pozo, Jose Angel Silva-Guillén, and Francisco Guinea**



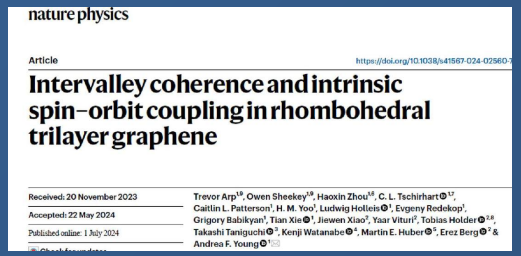




Name	Symbol	$\vec{p}$	Fermi surface	Legend
Isospin polarized states				
Fully symmetric	FS	$(\alpha,\alpha,\alpha,\alpha)$		
Half metal	HM	$(\alpha,0,\alpha,0)$		
Quarter metal	QM	$(\alpha,0,0,0)$		
Three-quarter metal	TQM	$(\alpha,\alpha,\alpha,0)$		
Partially isospin polarized states				
QM to HM	PIP_{11}	$(\alpha,\beta,0,0)$		
HM to FS	PIP_{22}	$(\alpha,\alpha,\beta,\beta)$		
HM to TQM	PIP_{21}	$(\alpha,\alpha,\beta,0)$		
QM to TQM	PIP_{12}	$(\alpha,\beta,\beta,0)$		
TQM to FS	PIP_{31}	$(\alpha,\alpha,\alpha,\beta)$		
QM to FS	PIP_{13}	$(\alpha,\beta,\beta,\beta)$		

- Same succession of unpolarized, half metal, and quarter metal phases in all systems
- Polarized phases stronger on the electron side
- Nematic phases, which break C_3, also possible
- Polarized phases favored by increased band splittings induced by the exchange term
- Trigonal warping leads to three hot spots at the Fermi surface, leading to p-wave SC

“Giant” spin-orbit coupling in rhombohedral graphite

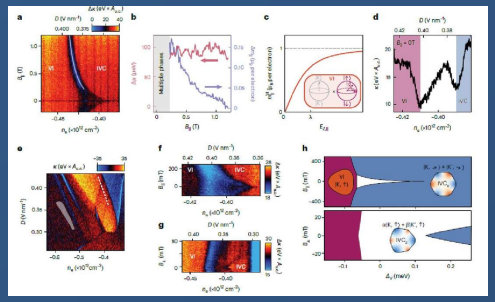

nature physics

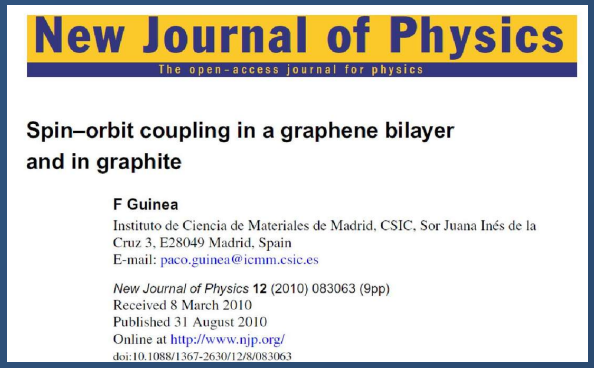
Article

Intervalley coherence and intrinsic spin–orbit coupling in rhombohedral trilayer graphene

Received: 20 November 2023
Accepted: 22 May 2024
Published online: 1 July 2024

Trevor Arp, Owen Sheekey, Haoxin Zhou, C. L. Tschirhart, Caitlin L. Patterson, H. M. Yoo, Ludwig Holleis, Evgeny Redekop, Grigory Babikyan, Tian Xie, Jiewen Xiao, Yaar Vituri, Tobias Holder, Takashi Taniguchi, Kenji Watanabe, Martin E. Huber, Erez Berg & Andrea F. Young

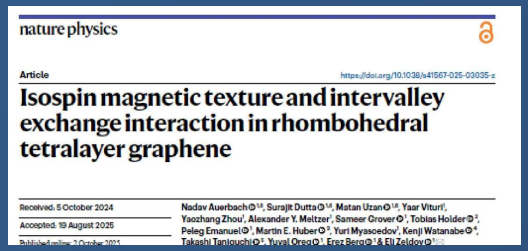



New Journal of Physics
The open-access journal for physics

Spin–orbit coupling in a graphene bilayer and in graphite

F Guinea
Instituto de Ciencia de Materiales de Madrid, CSIC, Sor Juana Inés de la Cruz 3, E28049 Madrid, Spain
E-mail: paco.guinea@icmm.csic.es

New Journal of Physics **12** (2010) 083063 (9pp)
Received 8 March 2010
Published 31 August 2010
Online at http://www.njp.org/
doi:10.1088/1367-2630/12/8/083063

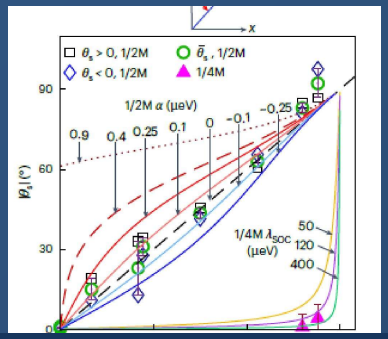

nature physics

Article

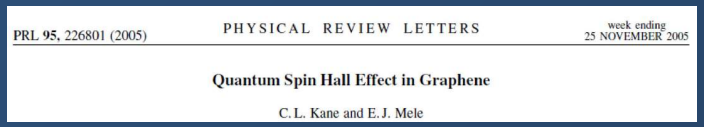
Isospin magnetic texture and intervalley exchange interaction in rhombohedral tetralayer graphene

Received: 5 October 2024
Accepted: 19 August 2025

Nadav Auerbach, Surajit Dutta, Matan Uzan, Yaar Vituri, Yaozhang Zhou, Alexander Y. Meltzer, Sameer Grover, Tobias Holder, Peleg Emanuel, Martin E. Huber, Yuri Myasoedov, Kenji Watanabe, Takashi Taniguchi, Yuval Oreg, Erez Berg & Eli Zeldov

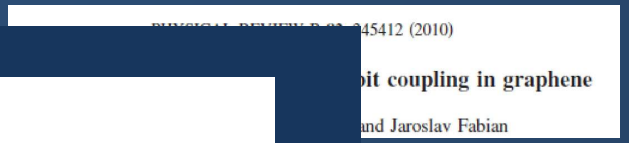


Spin Orbit Interaction in Graphite
G. Dresselhaus and M. S. Dresselhaus
Physical Review **140**, A401 (1965)


PRL 95, 226801 (2005) PHYSICAL REVIEW LETTERS week ending 25 NOVEMBER 2005

Quantum Spin Hall Effect in Graphene

C. L. Kane and E. J. Mele


45412 (2010)

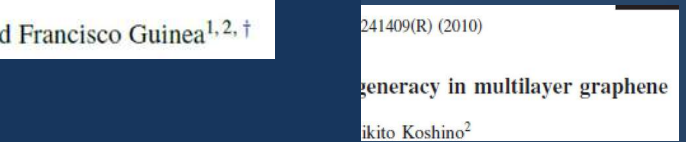
it coupling in graphene

nd Jaroslav Fabian


Intrinsic spin-orbit coupling in graphene stacks.

Guillermo Parra-Martinez,[1] Alejandro Jimeno-Pozo,[2] Ady Stern,[3] Jose Angel Silva-Guillén,[1,*] and Francisco Guinea[1,2,†]

arXiv:2610.05905


241409(R) (2010)

generacy in multilayer graphene

ikito Koshino[2]


pling in Bilayer Graphene

and Qing-feng Sun[1*]

arXiv:1004.0881

Spin-orbit in rhombohedral multilayers

Calculation including all *p* and *s* orbitals in the valence shell
Projection onto the p_z orbitals

In collaboration with A. Stern, G. Parra-Martínez, A. Jimeno-Pozo, J. Silva

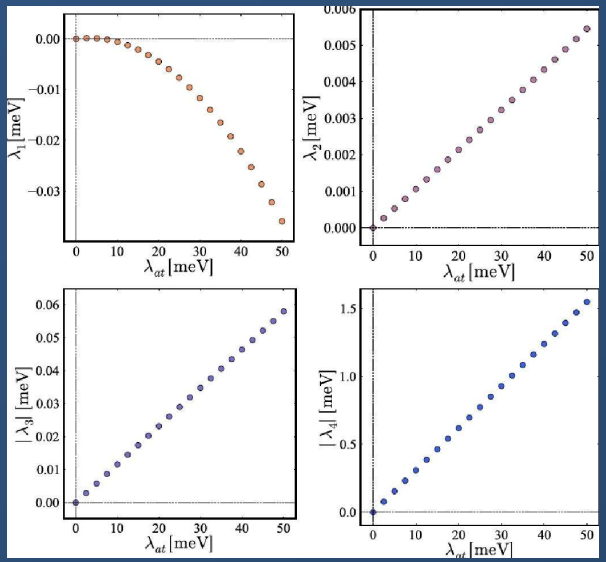
Atomic spin-orbit coupling $\mathcal{H}_{soc}^{at} = \lambda_{at} \sum_n \vec{L}_n \vec{s}_n$

Symmetry allowed terms

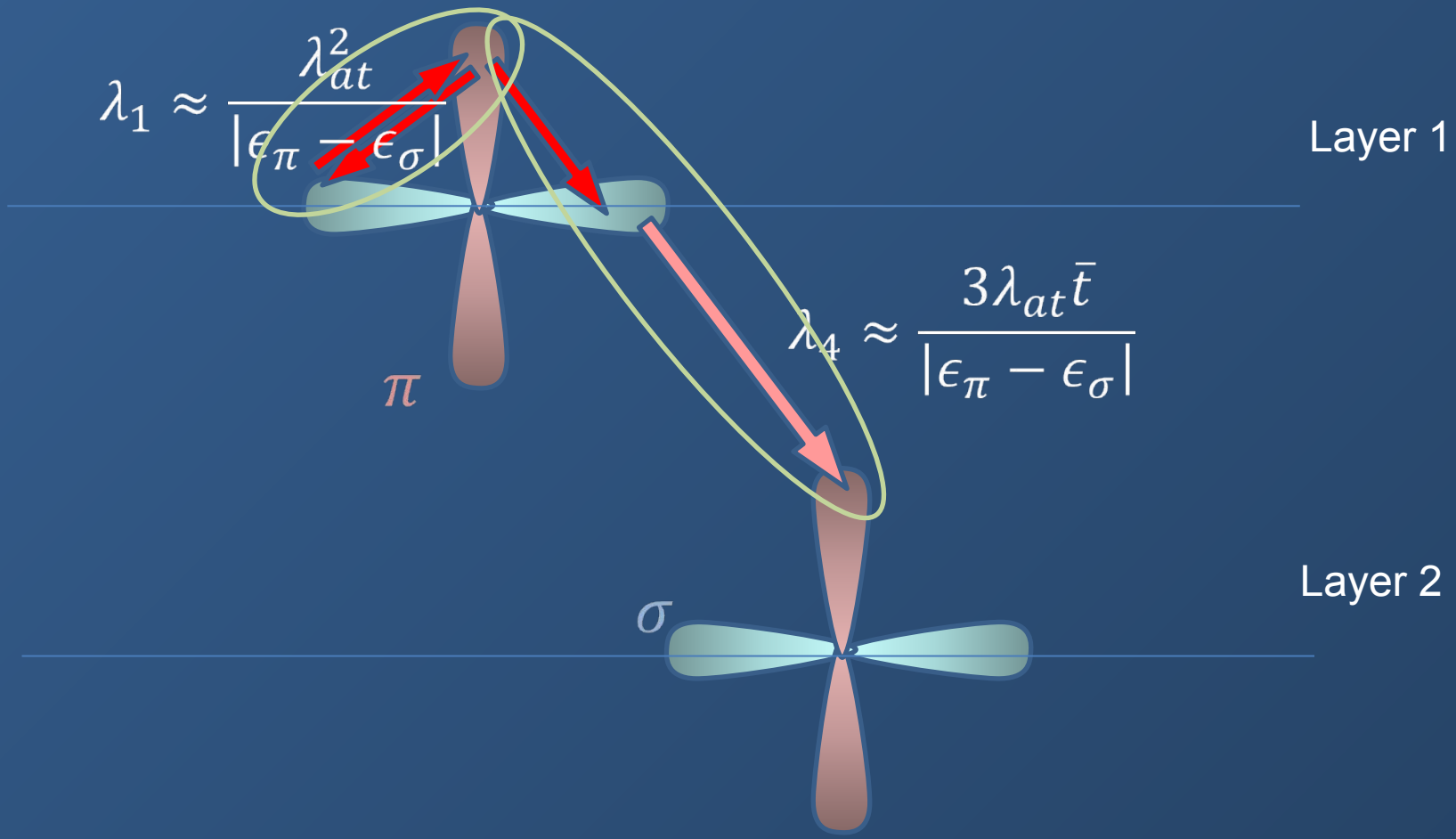
$$\mathcal{H}_{soc} = \sum_{n=1}^{n=N_L} \left[\lambda_1 \tau_z^n \sigma_z^n s_z^n + \lambda_2 (-1)^n \tau_z^n s_z^n + \lambda_3 (-1)^n \left(\sigma_y^n s_x^n - \tau_z^n \sigma_x^n s_y^n\right)\right] + \sum_{n=1}^{n=N_L-1} \lambda_4 \sigma_z^n \left(\mu_y^{n.n+1} s_x^n - \tau_z^n \mu_x^{n.n+1} s_y^n\right)$$

Kane Mele term

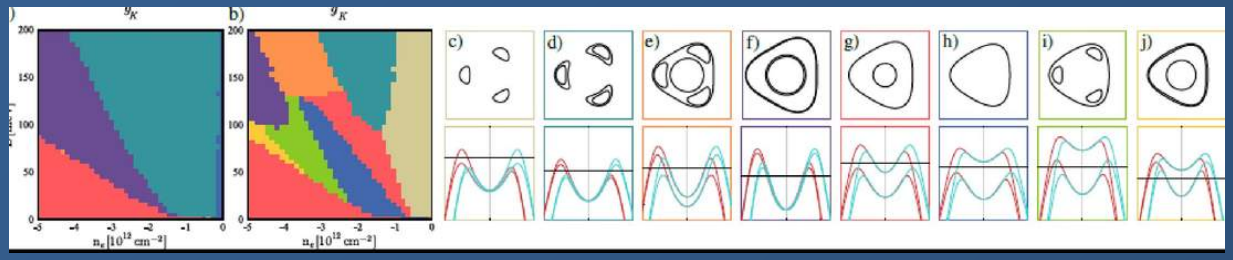
Spin flip+interlayer hopping



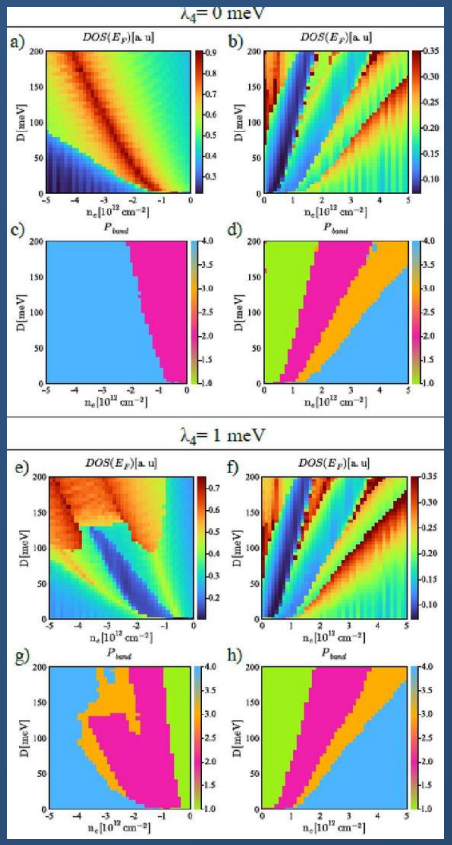
Spin orbit couplings: Kane-Mele, interlayer jump +spin flip



Fermi Surface topology, R4G



$\lambda_4 = 0$ $\lambda_4 = 1$ meV



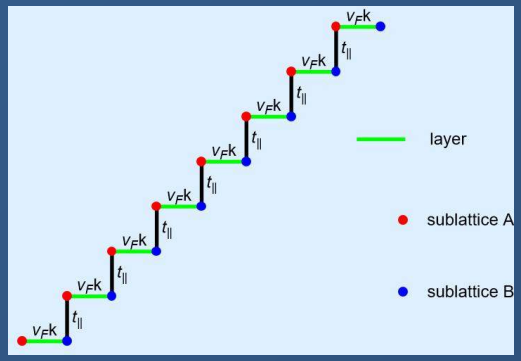
Hartree Fock phase diagram

Rhombohedral graphene. A toy model.

In collaboration with A. Bernevig and Y. Sao

Consider only the flat band of a semiinfinite stack (Berry trashcan approximation),

SSH approximation



Tight binding hamiltonian

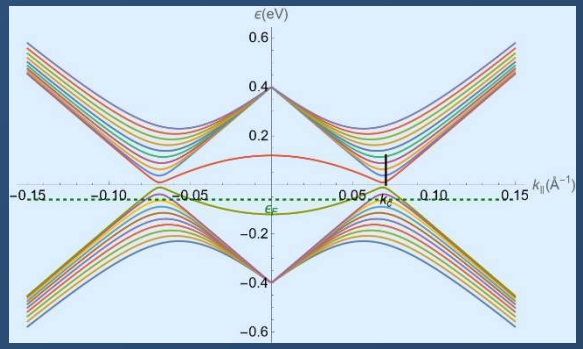
$$|\vec{k}\rangle = N^{-1/2} \sum_n \left(\frac{v_F k e^{i\phi_k}}{t_\parallel} \right)^n |n, A\rangle$$

Flat band dispersion

"Berry Trashcan" Model of Interacting Electrons in Rhombohedral Graphene

B. Andrei Bernevig[1,2,3] and Yves H. Kwan[4]

arXiv:2503.09692

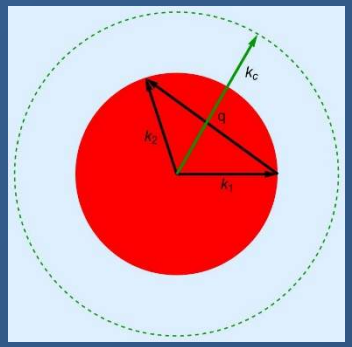


Bands with shift due to displacement field.
Approximate quadratic dispersion.

$$\epsilon_{\vec{k}} = \frac{\vec{k}^2}{2m^*}$$

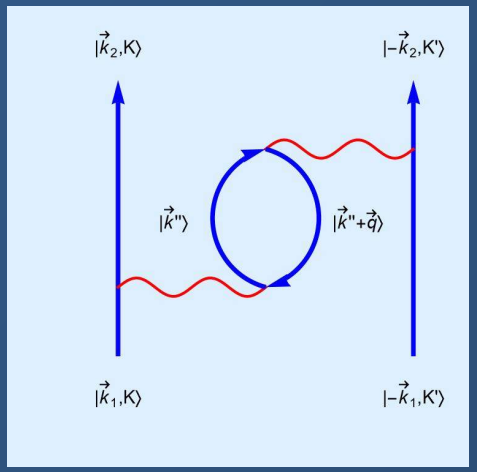
Pairing due to long range interactions (Kohn-Luttinger)

Fermi surface



Radius of the flat band:

$$k_c = \frac{v_F}{t_\parallel}$$



screened potential

$$v_{scr}(q) = \frac{v_0(q)}{1 + n_f v_0(q)\chi_0(q)} \approx \frac{1}{n_f \chi_0(q)}$$

susceptibility

$$\chi_0(q) = \sum_{\vec{k}''} \left|\left\langle \vec{k}'' \middle| \vec{k}'' + \vec{q} \right\rangle\right|^2 \frac{n_{\vec{k}''+\vec{q}} - n_{\vec{k}''}}{\epsilon_{\vec{k}''+\vec{q}} - \epsilon_{\vec{k}''}}$$

Linear equation for the gap

$$\Delta_l(T_c) \approx -\log\left(\frac{W}{T_c}\right)\lambda_l \Delta_l(T_c)$$

Gap at zero temperature

$$\Delta_l \approx W e^{-1/|\lambda_l|}$$

See also:

RESEARCH ARTICLE | AUGUST 13 2013

Superconductivity from repulsive interaction FREE

Saurabh Maiti; Andrey V. Chubukov

AIP Conf. Proc. 1550, 3–73 (2013)

https://doi.org/10.1063/1.4818400

How pairing mechanism dictates topology in valley-polarized superconductors with Berry curvature

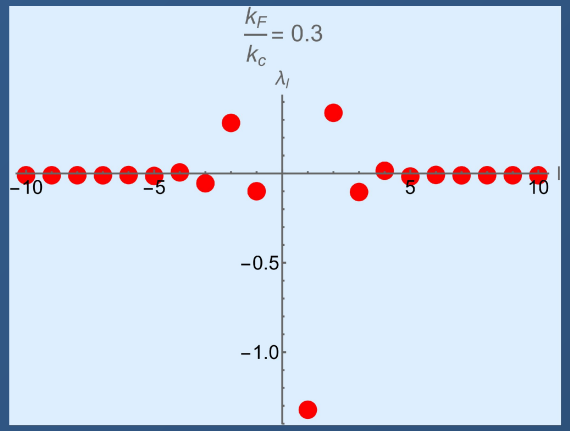
Julian May-Mann,* Tobias Helbig, and Trithep Devakul†

Dimensionless coupling constant

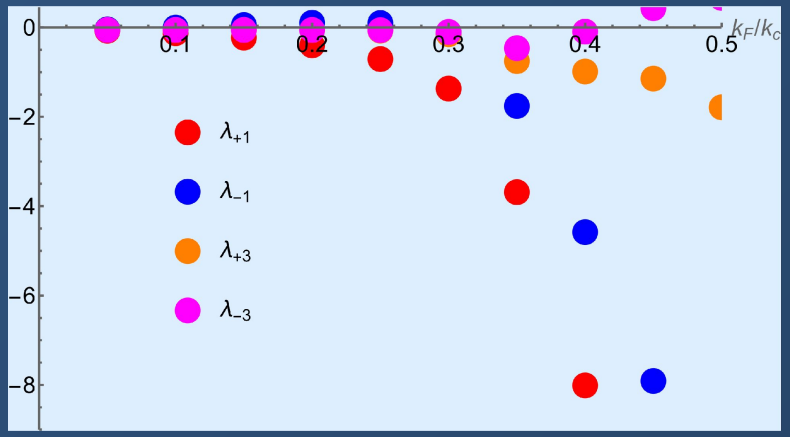
$$\lambda_l = \frac{\rho(\epsilon_F)}{2\pi}\int_0^{2\pi} d\theta\, e^{il\theta} \times \begin{Bmatrix} M_{K,K'}\left(\vec{k}_1,\vec{k}_2\right) \\ M_{K,K}\left(\vec{k}_1,\vec{k}_2\right) \end{Bmatrix} \times v_{scr}(q) \approx \frac{1}{2\pi}\int_0^{2\pi} d\theta\, e^{il\theta} \times \begin{Bmatrix} M_{K,K'}\left(\vec{k}_1,\vec{k}_2\right) \\ M_{K,K}\left(\vec{k}_1,\vec{k}_2\right) \end{Bmatrix} \times \frac{\chi_0(0)}{n_f \chi_0(q)}$$

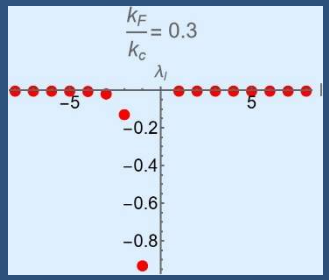
System dependent parameters, e^2, m^*, drop out, only dimensionless form factors remain

Quarter metal. Superconducting coupling constant

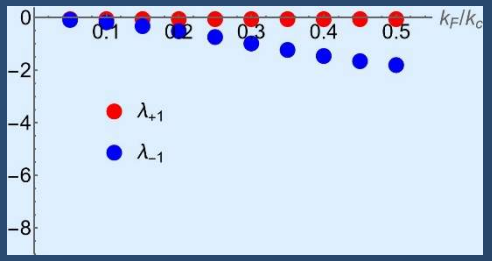


Screened Coulomb interaction





Negative Hubbard U



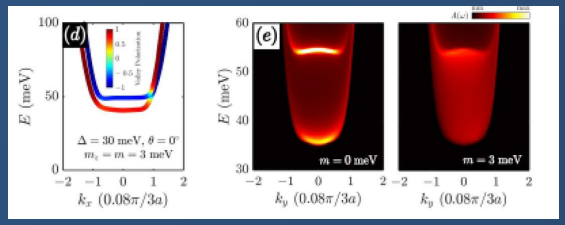
Domain walls in quarter metals

Reconfigurable chiral superconductivity

Surajit Dutta[1†], Nadav Auerbach[1†], Tonghang Han[2†], Yaozhang Zhou[1], Gal Shavit[3], Niladri-Sekhar Kander[1], Yuri Myasoedov[1], Martin E. Huber[4], Kenji Watanabe[5], Takashi Taniguchi[6], Long Ju[2#], and Eli Zeldov[1*]

arXiv:2605.13303

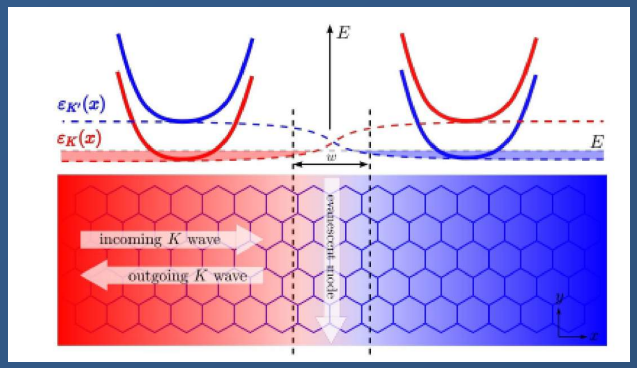
In collaboration with V. T. Phong, E. Mele, E. Prada, P. San-Jose, F. Lobo

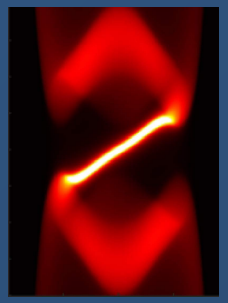


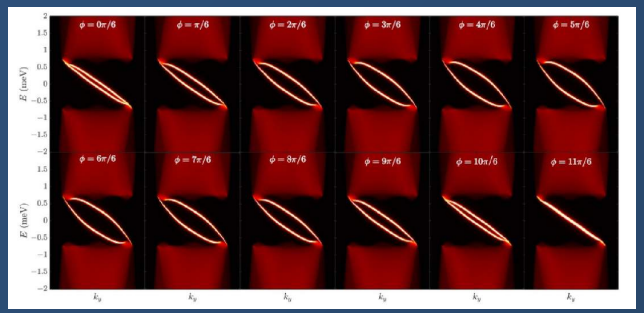
Electronic structure of the domain wall in the normal state.

The transmision vanishes unless:

- The barrier has the armchair orientation.
- There is intervalley coherence at the barrier.







Electronic structure of the domain wall in the superconducting state.

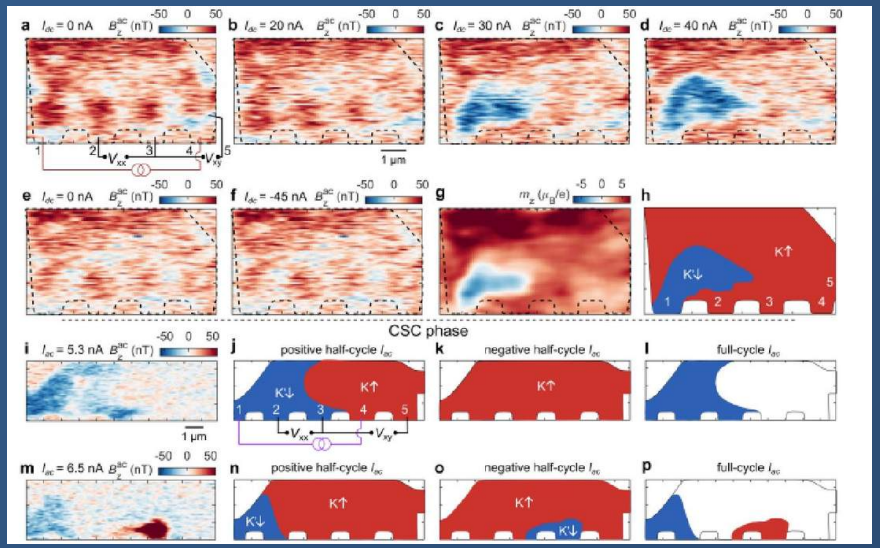
- Topological superconductivity.
- Existence of Majorana states.

Imaging valley magnetization and domain walls in real space

Reconfigurable chiral superconductivity

Surajit Dutta[1†], Nadav Auerbach[1†], Tonghang Han[2†], Yaozhang Zhou[1], Gal Shavit[3], Niladri-Sekhar Kander[1], Yuri Myasoedov[1], Martin E. Huber[4], Kenji Watanabe[5], Takashi Taniguchi[6], Long Ju[2#], and Eli Zeldov[1*]

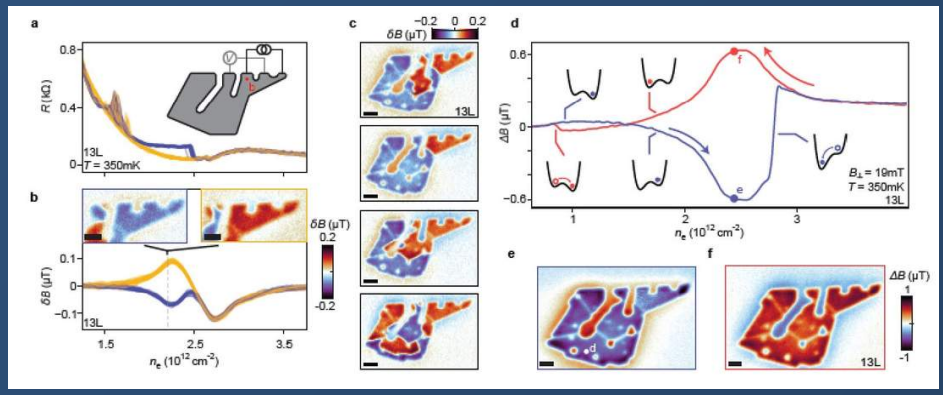
arXiv:2605.13303



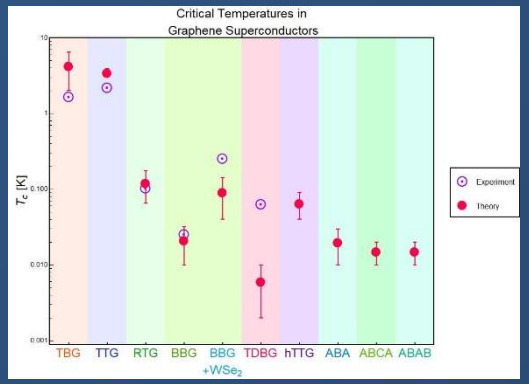
Visualizing orbital magnetism in electron doped rhombohedral multilayer graphene

Owen I. Sheekey,[1,*] Trevor B. Arp,[1,*] Benjamin A. Foutty,[1,*] Ruoxi Zhang,[1,*] Tixuan Tan,[2] Ludwig F. W. Holleis,[1] Yi Guo,[1] Sandesh S. Kalantre,[3,2] Canxun Zhang,[1] Mark Zakharyan,[1] David Gong,[1] Aidan Keough,[1] Youngjoon Choi,[1] Ysun Choi,[1] Siyuan Xu,[1] Tian Xie,[1] Ben Hodder Alexander,[3,2] Marisa Hocking,[4,3] Qingrui Cao,[3] Martin E. Huber,[5] Takashi Taniguchi,[6] Kenji Watanabe,[7] Chenhao Jin,[1] Étienne Lantagne-Hurtubise,[8] Aaron Sharpe,[3,2] Trithep Devakul,[2] and Andrea F. Young[1,†]

arXiv:2605.30316

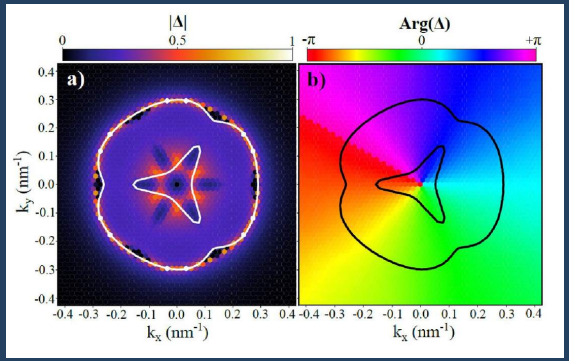


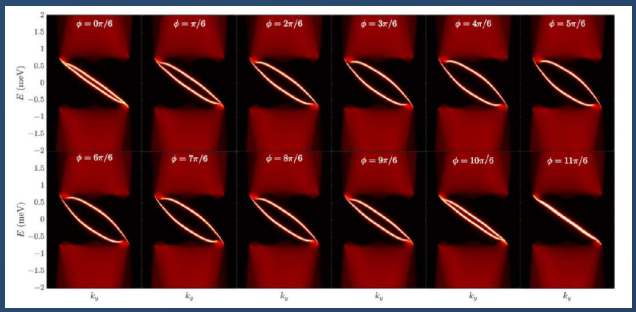
- The long range Coulomb interaction plays a major role in the electronic properties of graphene stacks.
- The main trends of the superconducting properties are reasonably described using standard parameters,



Electronic bands								Coulomb potential		Deformation potential and elastic constants		
2.46	5.253	0.4	0.32	0.044	0.05	0.797	0.0975	40	10	20	3.25	9.44

Rhombohedral graphene stacks show a rich electronic behavior all the way to the 3D limit







éctor
ainz-Cruz
mdea)



Tien Phong
enn, FSU)



s R. Walet
Manchester)



Guillermo Parra
Federico Escudero (UNS, Argentina)
Min Long (Wuhan U)
Alejandro Jimeno-Pozo
Zhen Zhan
Saul Herrera (UNAM, Mexico)
Adrian Ceferino
Pierre Pantaleon
Jose Silva
Hector Sainz-Cruz

Also:
L. Levitov (MIT)
L. Fu (MIT)
V. Crépel (MIT)
S. Yuan (Wuhan U.)
J. Lischner, (Imperial C.)
Z. Goodwin, (Imperial C.)
H. Rostami (Bath U.),
E. Cappelluti (Trieste)
D. Loo (NUS)
M. M. E. Alezzi (NUS)
S. Adam (NUS)
G. Vignale (NUS)
A. Stern (Weizmann)
R. Makov (Weizmann)
Y. Oreg (Weizmann)
P. Emanuel (Weizmann)
L. Glazman (Yale)
F. Von Oppen (Berlin)
E. Mele (U. Penn)
A. Bernevig (Priceton and DIPC)
Nemin Wei (Yale)

- Electronic charge fluctuations describe a pairing mechanism which is not suppressed by repulsive interactions. It is described by few adjustable parameters.
- The role of charge fluctuations is enhanced in systems with complex electronic wavefunctions, like twisted bilayer graphene. The strength of Umklapp processes correlates with the critical temperature.
- f-wave symmetry is a possible order parameter in twisted bilayer graphene.
- Superconductivity in a fully polarized is influenced by trigonal warping, and can be gapless.

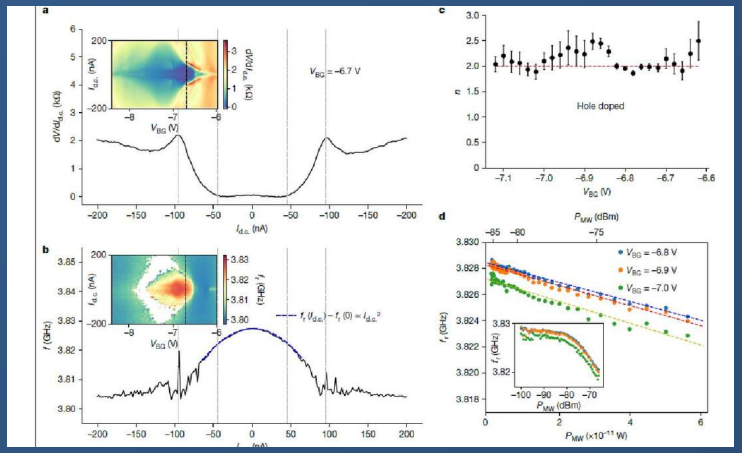
Superconducting stiffness: recent results

Superfluid stiffness of magic-angle twisted bilayer graphene

https://doi.org/10.1038/s41586-024-08494-7
Received: 17 June 2024
Accepted: 5 December 2024
Published online: 5 February 2025

Miuko Tanaka[1,2,9], Joel I-j. Wang[1,9] ✉, Thao H. Dinh[3], Daniel Rodan-Legrain[1], Sameia Zaman[1,4], Max Hays[1], Aziza Almanakly[1,4], Bharath Kannan[1,4,8], David K. Kim[5], Bethany M. Niedzielski[5], Kyle Serniak[1,5], Mollie E. Schwartz[5], Kenji Watanabe[6], Takashi Taniguchi[7], Terry P. Orlando[1,4], Simon Gustavsson[1,5], Jeffrey A. Grover[1], Pablo Jarillo-Herrero[3] ✉ & William D. Oliver[1,3,4] ✉

Nature **638**, **99** (2025)



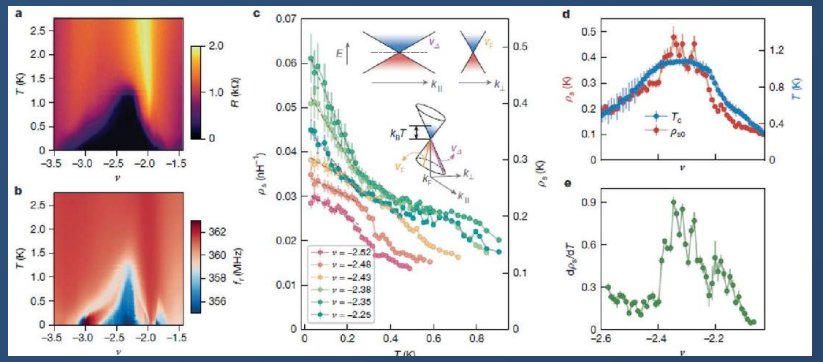
Article

Superfluid stiffness of twisted trilayer graphene superconductors

https://doi.org/10.1038/s41586-024-08444-3
Received: 19 June 2024
Accepted: 22 November 2024

Abhishek Banerjee[1,7], Zeyu Hao[1,7], Mary Kreidel[1,7], Patrick Ledwith[1], Isabelle Phinney[1], Jeong Min Park[2], Andrew Zimmerman[1], Marie E. Wesson[1], Kenji Watanabe[3], Takashi Taniguchi[4], Robert M. Westervelt[1], Amir Yacoby[1], Pablo Jarillo-Herrero[2], Pavel A. Volkov[1,5], Ashvin Vishwanath[1], Kin Chung Fong[6] ✉ & Philip Kim[1] ✉

Nature **638**, 93 (2025)



Superconducting stiffness: power law dependence on temperature

Pair breaking due to interlayer scattering

- Pair breaking due to intervalley scattering in a nodeless f-wave superconductor is equivalent to scattering by magnetic impurities in a conventional s-wave superconductor.

PHYSICAL REVIEW VOLUME 137, NUMBER 4A 15 FEBRUARY 1965

Theory of the Thermal Conductivity of Superconducting Alloys with Paramagnetic Impurities

VINAY AMBEGAOKAR* AND ALLAN GRIFFIN†

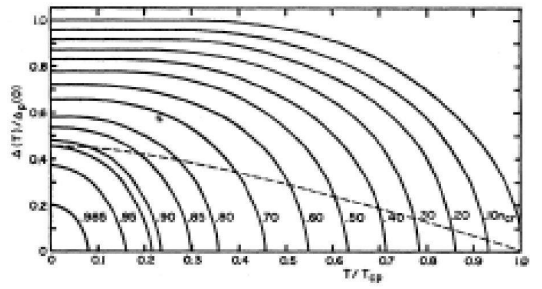


FIG. 4. The Gor'kov order parameter $\Delta(T,\tau_S)$ for a paramagnetic alloy (relative to its value in a pure metal at $T=0$°K) as a function of the temperature (relative to the transition temperature of a pure metal). The dashed curve is defined by $\Delta(T,\tau_S)\tau_S=1$, τ_S^{-1} being proportional to the impurity concentration n_i [see (2.26)]. For a given value of n_i, the gapless region occurs for temperatures $T_g \leq T < T_c$, where T_c is the transition temperature for that concentration and T_g is the temperature at which the dashed curve crosses $\Delta(T,n_i)$. The minimum value of n_i at which gaplessness occurs down to 0°K is $\exp(-\pi/4)n_{ic}\simeq 0.91 n_{ic}$, assuming the relation $\Delta_p(0)=1.76T_{cp}$. The curve for this concentration is not labeled.

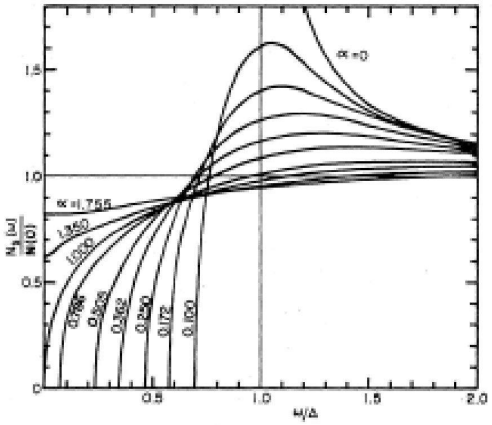


FIG. 6. The density of states $N_s(\omega)$ in a paramagnetic alloy function of the excitation frequency ω (we have normalized the former with respect to a normal metal and the latter with respect to the Gor'kov order parameter Δ). The density of states for nonmagnetic impurities is also shown $[\alpha \equiv (\tau_S\Delta)^{-1}=0]$.

- The relevant energy scales are the superconducting gap, Δ, and the scattering time due to intervalley processes, τ_{iv}.
- The superconducting phase is always gapless near the critical temperature.
- The superconductor is gapless at all temperatures if $\Delta(T=0) \leq \hbar/\tau_{iv}$.

Estimates: $\Delta(T=0)\sim 0.5$ meV, $v_F \sim v_F^G/50$, $\ell_{iv}\sim 50-500$ nm, $\hbar/\tau_{iv} \sim 0.02-0.2$ meV

Dissipation in TBG Josephson junctions

nature communications

Article

https://doi.org/10.1038/s41467-025-58325-0

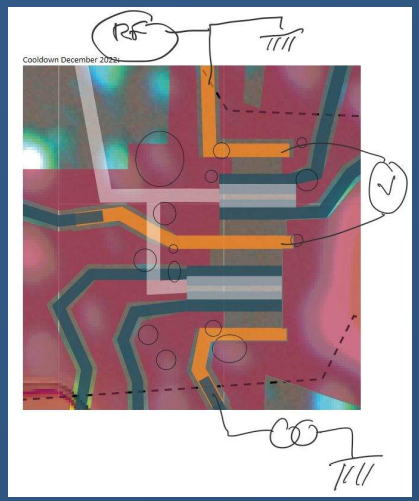
Quasiparticle and superfluid dynamics in Magic-Angle Graphene

Received: 15 October 2024

Accepted: 19 March 2025

Published online: 08 May 2025

Elias Portolés[1], Marta Perego[1], Pavel A. Volkov[2,3], Mathilde Toschini[1], Yana Kemna[1], Alexandra Mestre-Torà[1], Giulia Zheng[1], Artem O. Denisov[1], Folkert K. de Vries[1], Peter Rickhaus[1], Takashi Taniguchi[4], Kenji Watanabe[5], J. H. Pixley[6,7], Thomas Ihn[1,8] & Klaus Ensslin[1,8]



$$I_c \approx 10\ nA$$
$$C = 32\ fF$$
$$R = 2.5\ k\Omega$$
$$\omega_p/2\pi = 4.9\ GHz$$
$$T \approx 10\ mK$$

$$E_J \approx 0.021\ meV$$
$$E_C \approx 0.0025\ meV$$
$$\hbar\omega_p \approx 0.02\ meV$$
$$Q \approx 2.5$$

Quantum effects

$$H = E_C\hat{Q}^2 + E_J\frac{\hat{\phi}^2}{2}$$

$$[\hat{Q}, \hat{\phi}] = 2i$$
$$\hat{Q} = 2i\partial_\phi$$

$$\psi(\phi) = \frac{2}{\sqrt{\pi}}\left(\frac{2E_C}{E_J}\right)^{1/4} e^{-\frac{1}{4}\sqrt{\frac{E_J}{2E_C}}\phi^2}$$

$$\langle\phi^2\rangle = \sqrt{\frac{8E_C}{E_J}}$$

$$\langle\phi^2\rangle \approx 0.99$$

"Berry Trashcan" Model of Interacting Electrons in Rhombohedral Graphene

B. Andrei Bernevig[1,2,3] and Yves H. Kwan[4]

arXiv:2503.09692

